

Automatic nonlinear MPC approximation with closed-loop guarantees

Abdullah Tokmak^{1,2,3}, Christian Fiedler², Melanie N. Zeilinger³, Sebastian Trimpe², Johannes Köhler³

Abstract—Safety guarantees are vital in many control applications, such as robotics. Model predictive control (MPC) provides a constructive framework for controlling safety-critical systems, but is limited by its computational complexity. We address this problem by presenting a novel algorithm that automatically computes an explicit approximation to nonlinear MPC schemes while retaining closed-loop guarantees. Specifically, the problem can be reduced to a function approximation problem, which we then tackle by proposing ALKIA-X, the Adaptive and Localized Kernel Interpolation Algorithm with eXtrapolated reproducing kernel Hilbert space norm. ALKIA-X is a non-iterative algorithm that ensures numerically well-conditioned computations, a fast-to-evaluate approximating function, and the guaranteed satisfaction of any desired bound on the approximation error. Hence, ALKIA-X automatically computes an explicit function that approximates the MPC, yielding a controller suitable for safety-critical systems and high sampling rates. We apply ALKIA-X to approximate two nonlinear MPC schemes, demonstrating reduced computational demand and applicability to realistic problems.

Index Terms—NL predictive control; Kernel-based function approximation; Machine learning; Constrained control

I. INTRODUCTION

MODEL predictive control (MPC) [1] is an optimization-based control method for nonlinear constrained systems, in which the applied control input is implicitly defined by the solution of a nonlinear program (NLP). Hence, online application of MPC under real-time requirements is challenging for fast applications like robotics. This has motivated extensive research on approximate MPC schemes [2]–[19] to obtain controllers suitable for high sampling rates. Specifically, these approaches approximate the MPC offline, i.e., prior to applying the controller. This offline approximation should ideally be automatic to simplify its application. Furthermore, the approximate MPC should retain closed-loop guarantees regarding stability and constraint satisfaction to allow for application on safety-critical systems.

Figure 1 outlines the proposed approach. We consider a *robust* MPC formulation [20]–[23], which is designed such that the desired closed-loop guarantees remain valid under input disturbances below a user-chosen error bound $\epsilon > 0$.

This work has been supported by the Swiss National Science Foundation under NCCR Automation (grant agreement 51NF40 180545), the IDEA League, and the German Academic Scholarship Foundation.

¹Department of Electrical Engineering and Automation, Aalto University, 02150 Espoo, Finland, abdullah.tokmak@aalto.fi.

²Institute for Data Science in Mechanical Engineering, RWTH Aachen University, 52068 Aachen, Germany, [christian.fiedler, trimpe}@dsme.rwth-aachen.de](mailto:{christian.fiedler, trimpe}@dsme.rwth-aachen.de).

³Institute for Dynamic Systems and Control, ETH Zurich, Zurich CH-8092, Switzerland, [mzeilinger, jkoehle}@ethz.ch](mailto:{mzeilinger, jkoehle}@ethz.ch).

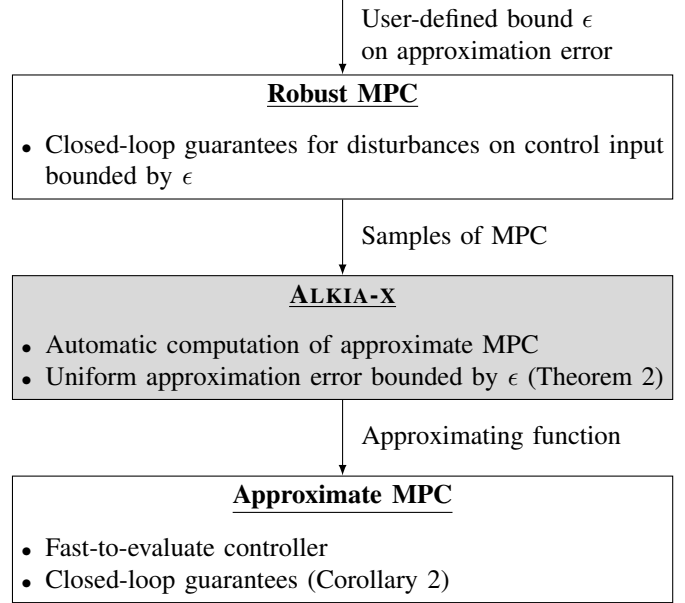


Fig. 1. A high level illustration of the proposed framework for approximate MPC with closed-loop guarantees. ALKIA-X automatically computes an explicit function that approximates a robust MPC scheme up to any specified accuracy ϵ , which yields a fast-to-evaluate approximate MPC with closed-loop guarantees. Notably, the proposed process is *non-iterative* due to the uniform error bounds inherently guaranteed by ALKIA-X.

By approximating the feedback law implicitly defined by this MPC up to a tolerance ϵ , the approximate MPC preserves all control-theoretic guarantees induced by the MPC. Hence, approximating the MPC can be cast as a function approximation problem by sampling state and corresponding optimal inputs obtained by solving the MPC offline. To address this function approximation problem, we propose ALKIA-X, the Adaptive and Localized Kernel Interpolation Algorithm with eXtrapolated reproducing kernel Hilbert space (RKHS) norm. ALKIA-X automatically computes an explicit function that approximates the MPC with a uniform approximation error ϵ , resulting in a cheap-to-evaluate approximate MPC with guarantees on stability and constraint satisfaction.

Related work: Linear MPC schemes can be exactly characterized as an explicit piecewise affine function over a polyhedral partition of the domain, which is known as explicit MPC [24], [25]. However, this exact solution tends to suffer from scalability issues, which has motivated research on approximate explicit MPC schemes. In [26], the domain is partitioned into hypercubes and the MPC is approximated using piecewise affine functions. Notably, [26, Lemma 1] ensures

that the approximate MPC respects the constraints by using a constrained optimization problem that leverages convexity. A similar approximate MPC is suggested in [27], using a more general continuous interpolation on each hypercube. However, these approaches primarily rely on convexity, and hence cannot be applied to nonlinear MPC schemes.

An overview of explicit MPC for nonlinear systems is given in [28]. A very appealing approach is to treat the MPC as a black-box function and use supervised machine learning techniques to obtain an explicit approximation. Approximating MPC schemes with neural networks (NNs) is a particularly popular approach [2]–[10], which was first suggested in [11]. However, it is difficult to ensure that the resulting NN provides desirable closed-loop properties, see the recent review paper [12]. One solution to this problem is adding a safety filter to change the output of the NN [2]–[6]. For linear systems, this can be achieved with a projection on a robust control invariant set [2], [3] or by using additional active set iterations [4]. For general nonlinear systems, an implicit safety filter can be obtained by validating the safety of the NN policy online and using an MPC-intrinsic fallback in case of predicted constraint violations [5], see also [6]. Other solutions include a posteriori safety validations of the NN using statistical validation [7].

A constructive approach to obtain closed-loop guarantees under approximation errors is to leverage *robust* MPC design methods [20]–[23]. For instance, [8]–[10] first design an MPC scheme that is robust with respect to input disturbances bounded by ϵ and then use NNs to approximate this MPC with an approximation error smaller than ϵ . However, guaranteeing the desired approximation error bound for NNs is challenging. In [8], [9], this issue is addressed by using statistical tools to validate the approximation accuracy with high probability. Nevertheless, this separate validation yields a nontrivial offline design consisting of multiple iterations between training the NN and validating its approximation.

A natural solution to this problem are nonparametric regression tools, such as kernel-based methods [18], [19], [29]–[43] or set-membership identification [13]–[16], [44], [45], which both provide error bounds. Nonparametric set-membership estimation typically assumes Lipschitz continuity and builds a non-falsified piecewise affine set that contains the ground truth, which is also called Kinky inference [44] or Lipschitz interpolation [45]. Applications of such tools to approximate nonlinear MPC schemes are explored in [13]–[16]. Similarly, in [17], a known Lipschitz bound is utilized to approximate an MPC with guaranteed error bound ϵ , using instead a quasi-interpolation approach. Kernel-based methods, such as kernel ridge regression (KRR) [29]–[33] or Gaussian process (GP) regression [18], [19], [33]–[43], enable smooth approximations and error bounds, assuming the ground truth lies in the corresponding RKHS. Applications of GPs to approximate MPC schemes are, e.g., explored in [18], [19], where closed-loop guarantees on the approximate MPC are provided using a posteriori sampling, similar to [8], [9]. These nonparametric estimation methods can in principle achieve any desired approximation accuracy ϵ , however, they are in general not computationally cheap-to-evaluate. In particular, the complexity of evaluating kernel-based approximations scales cubically in the

number of samples [34, Section 2.3], making it challenging to use for control applications. For kernel-based methods, computationally cheap online evaluation can, e.g., be ensured by only considering nearest-neighbor samples for the online evaluation [35, Section 4.A] or by iteratively dividing the input space and using local GPs [36], [37].

Overall, most state-of-the-art methods lack closed-loop guarantees, are limited to linear systems, yield computationally expensive approximate controllers, or require an iterative design process using a posteriori validation of error bounds.

Contribution: In this work, we present ALKIA-X, a novel algorithm based on kernel interpolation [30]–[33], a noise-free special case of KRR, to automatically approximate functions up to any desired accuracy. Hence, ALKIA-X enables the automatic approximation of nonlinear MPC schemes with closed-loop guarantees (see Figure 1). ALKIA-X has the following properties:

- (P1) Fast-to-evaluate approximating function;
- (P2) Guaranteed satisfaction of desired approximation error;
- (P3) Bound on worst-case number of required samples;
- (P4) Automatic and non-iterative algorithm with well-conditioned computations and ready-to-use Python implementation.¹

Property (P1) enables the implementation of the approximate MPC for fast control applications with limited computational resources. Property (P2) ensures closed-loop guarantees on stability and constraint satisfaction on the approximate MPC and is the main theoretical contribution in combination with (P3). Properties (P3) and (P4) enable a reliable and automatic approximation. The aforementioned properties are obtained by developing, extending, and combining the following tools:

- (T1) Localized kernel interpolation;
- (T2) Adaptive sub-domain partitioning and length scale adjustment;
- (T3) RKHS norm extrapolation.

Specifically, we follow a localized kernel interpolation approach (T1) by only using a subset of data, resulting in a piecewise-defined approximating function. Additionally, we adaptively partition the domain into sub-domains (T2), adjust the length scale accordingly, and sample equidistantly in each sub-domain. Finally, we derive a heuristic RKHS norm extrapolation (T3), eliminating the need for an oracle to provide the RKHS norm.

Overall, ALKIA-X successfully addresses the problem of approximating nonlinear MPC schemes with closed-loop guarantees by yielding a fast-to-evaluate approximating function (P1) and guaranteeing any desired approximation accuracy (P2) with a reliable and automatic algorithm (P3), (P4). We demonstrate the performance of ALKIA-X by approximating the MPC schemes for two nonlinear systems:

- 1) A simple continuous stirred tank reactor from prior work [8]. ALKIA-X computes the approximate MPC in 9h, yielding a controller with closed-loop guarantees and an online evaluation time below 50 μ s, thus outperforming prior work [8] by over one order of magnitude.

¹The code can be found here: <https://github.com/tokmaka1/ALKIA-X>

- 2) A realistic application to control a cold atmospheric plasma device [46, Chapter 4.5]. ALKIA-X computes the approximate MPC in 66 h, yielding a controller with only 33 MB of memory and an online evaluation time of 100 μ s.

Outline: We present the problem setting in Section II-A, where we formally reduce the MPC approximation problem into a function approximation problem. We use kernel interpolation to tackle the function approximation problem, for which we introduce preliminaries in Section II-B. Section III introduces the adaptive and localized kernel interpolation algorithm, including theoretical guarantees regarding the desired approximation error and worst-case sample complexity. Section IV extends the approach to unknown RKHS norms by using an RKHS norm extrapolation, yielding ALKIA-X. Furthermore, Section V investigates approximating MPC schemes via ALKIA-X and the resulting closed-loop guarantees on the approximate MPC. Section VI demonstrates the successful deployment of ALKIA-X for approximating two nonlinear MPC schemes. Finally, we conclude the paper in Section VII.

Notation: The set of non-negative real numbers is given by $\mathbb{R}_{\geq 0}$. The set of positive real numbers and the set of natural numbers greater or equal to $N \in \mathbb{R}_{\geq 0}$ are denoted by $\mathbb{R}_{> 0}$ and $\mathbb{N}_{\geq N}$, respectively. For a set $X \subseteq \mathbb{R}^N$, we denote the cardinality by $\text{card}(X)$. For a vector $x \in \mathbb{R}^n$, the Euclidean norm, the infinity norm, and the 1-norm are denoted by $\|x\|_2$, $\|x\|_\infty$, and $\|x\|_1$, respectively. For a matrix $A \in \mathbb{R}^{n \times n}$, the induced infinity norm is denoted by $\|A\|_\infty$. We define $\mathbf{1}_n = [1, \dots, 1]^\top \in \mathbb{R}^n$ and $\mathbf{0}_n = [0, \dots, 0]^\top \in \mathbb{R}^n$. For two functions $f: \mathbb{R}_{\geq 0} \rightarrow \mathbb{R}_{\geq 0}$ and $g: \mathbb{R}_{\geq 0} \rightarrow \mathbb{R}_{\geq 0}$, we write $f(\epsilon) = \mathcal{O}(g(\epsilon))$ if $\frac{f(\epsilon)}{g(\epsilon)} < \infty$ as $\epsilon \rightarrow 0$ with $\epsilon > 0$. Moreover, a function $f: \mathbb{R}_{\geq 0} \rightarrow \mathbb{R}_{\geq 0}$ belongs to class \mathcal{K}_∞ if it is strictly increasing, continuous, and $f(0) = 0$.

II. PROBLEM SETTING AND PRELIMINARIES

First, we describe the problem setting (Section II-A) before giving preliminaries on kernel interpolation (Section II-B). Then, we discuss the computation of an upper bound on the power function (Section II-C).

A. Problem setting

We consider a general nonlinear dynamical system $x_{t+1} = g(x_t, u_t)$ with system state $x_t \in \mathbb{R}^n$, control input $u_t \in \mathbb{R}^{n_u}$, and time index $t \in \mathbb{N}$. The control goal is to stabilize the steady-state x_s while ensuring the satisfaction of user-specified state and input constraints, i.e., $x_t \in \mathcal{X} \subseteq \mathbb{R}^n$, $u_t \in \mathcal{U} \subseteq \mathbb{R}^{n_u}$, $\forall t \in \mathbb{N}$. MPC provides a constructive approach to define a feedback law $u = f(x)$ that ensures asymptotic stability and constraint satisfaction.

Approximate MPC: The feedback law f is based on the solution of a finite-horizon optimal control problem and solving such an NLP during online operation is computationally expensive. Hence, we aim to replace f with an explicit approximate feedback law $u = h(x)$ that we construct offline. The main challenge is to ensure that the approximate MPC h inherits the closed-loop guarantees induced by the MPC f .

Solution approach: The proposed framework is outlined in Figure 1. Analogous to the approach in [8], [9], we consider an MPC feedback law f that is robust with respect to input disturbances bounded by ϵ . Hence, the approximate MPC yields desirable closed-loop guarantees if $\|f(x) - h(x)\|_\infty \leq \epsilon$ for all $x \in \mathcal{X}$.

Function approximation: Consequently, the problem of determining an approximate MPC with closed-loop guarantees reduces to computing an explicit function h that approximates the ground truth f with a uniform approximation error bounded by ϵ , i.e., $\|f(x) - h(x)\|_\infty \leq \epsilon$ for all $x \in \mathcal{X}$. The ground truth f is implicitly defined through the solution of an NLP, and hence we regard f as a black-box function that we can query to receive noise-free evaluations. In the following, we focus solely on this general function approximation problem. Specifically, in this paper, we solve this function approximation problem by proposing a novel algorithm based on kernel interpolation. We revisit the resulting control properties of the approximate MPC scheme later in Section V.

Simplifications: We consider, w.l.o.g., a scalar ground truth $f: \mathcal{X} \rightarrow \mathbb{R}$ and approximating function $h: \mathcal{X} \rightarrow \mathbb{R}$, and thus require

$$|f(x) - h(x)| \leq \epsilon \quad \forall x \in \mathcal{X}. \quad (1)$$

For vector-valued functions, each output dimension can be approximated individually, resulting in multiple scalar approximation problems ensuring $\|f(x) - h(x)\|_\infty \leq \epsilon$ for all $x \in \mathcal{X}$. For simplicity of exposition, we assume that the domain is a unit cube, i.e., $\mathcal{X} = [0, 1]^n$.

B. Preliminaries on kernel interpolation

In this section, we introduce kernel interpolation, see [30]–[33] for more details. First, we collect the standing assumptions on the kernel $k: \mathcal{X} \times \mathcal{X} \rightarrow \mathbb{R}_{> 0}$, which is the central object in kernel interpolation.

Assumption 1. *The kernel k is*

- 1) *continuous.*
- 2) (strictly) $\begin{matrix} \text{positive} & \text{definite,} \\ \text{i.e., } \sum_{i=1}^N \sum_{j=1}^N \alpha_i \alpha_j k(x_i, x_j) & > 0 \text{ for all} \\ \mathbb{R}^N \ni [\alpha_1, \dots, \alpha_N]^\top \neq \mathbf{0}_N, & \text{for all pairwise distinct} \\ x_1, \dots, x_N \in \mathcal{X}, \text{ and any } N \in \mathbb{N}. \end{matrix}$
- 3) *only a function of the Euclidean distance, i.e., $\exists \tilde{k}: \mathbb{R}_{\geq 0} \rightarrow (0, 1]$ such that $k(x, x') = \tilde{k}(\|x - x'\|_2)$ for all $x, x' \in \mathcal{X}$. Moreover, \tilde{k} is strictly decreasing and $\tilde{k}(0) = 1$.*

The first two conditions in Assumption 1 are standard assumptions for kernels [30]. Condition 3) implies a uniform length scale in all dimensions and that k is a radial kernel [31, Chapter 4.7]. We can assume $\tilde{k}(0) = 1$ w.l.o.g. by normalizing. Assumption 1 holds for many common kernels, such as the squared-exponential or the Matérn kernel [34].

Let $X = \{x_1, \dots, x_N\} \subseteq \mathcal{X}$ be a set of samples and assume that x_1, \dots, x_N are pairwise distinct. We collect the noise-free evaluations of f on the inputs X in a vector denoted by

$$f_X = [f(x_1), \dots, f(x_N)]^\top. \quad (2)$$

Given samples X , we denote by $K_X \in \mathbb{R}_{> 0}^{N \times N}$ the symmetric and positive definite covariance matrix, also known as the

kernel matrix or the Gram matrix [31], [34], i.e., the entry at row i and column j is $k(x_i, x_j)$ for any $i, j \in \{1, \dots, N\}$. Given samples X , the covariance vector $k_X: \mathcal{X} \rightarrow \mathbb{R}_{>0}^N$ is defined as

$$k_X(x) := [k(x, x_1), k(x, x_2), \dots, k(x, x_N)]^\top. \quad (3)$$

With the introduced definitions, we can write the resulting approximating function $h_X: \mathcal{X} \rightarrow \mathbb{R}$ as [33, Section 3.2]

$$h_X(x) = f_X^\top K_X^{-1} k_X(x). \quad (4)$$

The RKHS norm is a characteristic value of RKHS functions that quantifies their complexity, and which we later use to bound the approximation error. We denote the RKHS norm of a function with respect to the RKHS of kernel k by $\|\cdot\|_k$ and the RKHS norm of the approximating function (4) satisfies

$$\|h_X\|_k = \sqrt{f_X^\top K_X^{-1} f_X}. \quad (5)$$

Notably, approximating function (4) is the unique solution of a variational problem [33, Theorem 3.5], interpolating the given samples, i.e., $h_X(x) = f(x)$ for all $x \in X$, with the minimal RKHS norm. Thus, $\|f\|_k \geq \|h_X\|_k$ holds for all $X \subseteq \mathcal{X}$. Henceforth, we assume that the unknown ground truth f is a member of the RKHS of the chosen kernel k , which trivially implies $\|f\|_k < \infty$. This is a standard assumption for kernel-based approximation (see e.g., [29], [30], [38]–[43]), which we discuss in more detail later (see Assumptions 3 and 5).

Next, we define the power function $P_X: \mathcal{X} \rightarrow [0, 1]$ [32, Section 9.3]

$$P_X(x) := \sqrt{1 - k_X(x)^\top K_X^{-1} k_X(x)}, \quad (6)$$

which is used in the following proposition to characterize input-dependent error bounds for kernel interpolation.

Proposition 1. [32, Section 14.1] *Let Assumption 1 hold. Then, we have*

$$|f(x) - h_X(x)| \leq P_X(x) \sqrt{\|f\|_k^2 - \|h_X\|_k^2} \quad (7)$$

for all $x \in \mathcal{X}$ and any samples $X \subseteq \mathcal{X}$.

Note that Proposition 1 is a modified version of the Golomb-Weinberger bound [32, Section 9.3]. Based on Proposition 1, we can obtain *uniform* bounds on the approximation error given a uniform upper bound on the power function P_X and the ground truth RKHS norm $\|f\|_k$. Additionally, the following lemma ensures continuity of the RKHS function.

Lemma 1. *Let Assumption 1 hold. Then, for all $x, x' \in \mathcal{X}$, we have*

$$|f(x) - f(x')| \leq \|f\|_k \sqrt{2\mathfrak{K}(\|x - x'\|_2)} \quad (8)$$

with

$$\mathfrak{K} := 1 - \tilde{k} \in \mathcal{K}_\infty.^2 \quad (9)$$

The proof can be found in Appendix A. Lemma 1 later assists in proving sample complexity bounds for arbitrarily accurate approximating functions.

²Due to Assumption 1, the function $\mathfrak{K}: \mathbb{R}_{\geq 0} \rightarrow [0, 1)$ belongs to class \mathcal{K}_∞ , and thus its inverse $\mathfrak{K}^{-1}: [0, 1) \rightarrow \mathbb{R}_{\geq 0}$ is a continuous and strictly increasing function, i.e., it is again a class \mathcal{K}_∞ function [47, Lemma 4.2].

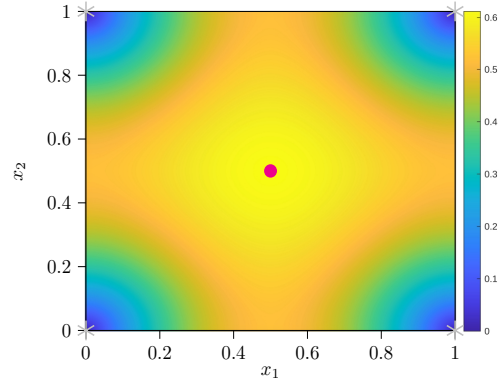


Fig. 2. Power function P_X on a cube with samples X on its vertices, which are illustrated by the gray asterisks. The maximum of the power function is at the center and is highlighted by the magenta point. This plot is generated with the Matérn kernel with $\nu = 3/2$ to compute the power function on the cube $[0, 1]^2$.

C. Upper bound on the power function

Based on (7), we can ensure the desired uniform error bound (1) if a bound on the RKHS norm of the ground truth and a uniform upper bound on the power function P_X are available. However, finding the maximum of P_X over the space \mathcal{X} in general requires the solution of a non-convex optimization problem. We circumvent this issue by using a local approximation scheme with samples X at the 2^n vertices of a cube. In this symmetric setting, the center of the cube is the farthest away from the given samples. Since *radial* kernels (see Assumption 1) are strictly decreasing functions of the Euclidean distance between two inputs, it is reasonable to assume that the maximum of the power function is at the center of the cube.

Assumption 2. *For any cube $\tilde{\mathcal{X}} \subseteq \mathcal{X}$ with 2^n samples X located at its vertices and with the center $\bar{x} = \frac{1}{2^n} \sum_{x \in X} x$, it holds that $P_X(x) \leq P_X(\bar{x})$ for all $x \in \tilde{\mathcal{X}}$.*

Figure 2 shows an exemplary power function, highlighting that the maximum of the power function is indeed at the center of the cube.

III. ADAPTIVE AND LOCALIZED KERNEL INTERPOLATION ALGORITHM

In this section, we present the proposed adaptive and localized kernel interpolation algorithm to automatically compute a sufficiently accurate approximating function. In Section III-A, we describe the main idea before explaining the details in Section III-B. We provide a theoretical analysis in Section III-C, including the guaranteed error bound and a bound on the worst-case sample complexity.

A. Main idea

A naïve approach to determine a sufficiently accurate approximating function would be to equidistantly sample the ground truth until the kernel interpolation ensures the desired error bound (1). The proposed approach modifies classic kernel

interpolation by using *local* approximations and an *adaptive* adjustment of the length scale.

We use a *localized* kernel interpolation approach (T1) by locally sampling equidistantly and computing a piecewise-defined approximating function based on local cubes that only use a subset of the available samples. This results in a fast online evaluation (P1), a highly parallelized offline approximation, and enables the reliable computation of a guaranteed bound on the approximation error (P2), (P3).

Additionally, we use an *adaptive* adjustment of the length scale by partitioning the domain into sub-domains (T2) and perform localized kernel interpolation on each sub-domain separately, where each sub-domain has an individual length scale and RKHS norm. For every sub-domain, we can compute the sufficient number of samples that ensure an approximation error that is uniformly bounded by ϵ . Moreover, we impose an upper bound on the number of samples per sub-domain using a hyperparameter $\bar{p} \in \mathbb{N}$. If more samples are required to ensure the desired error bound, we partition the sub-domain and reduce the length scale. This leads to an *adaptive* sub-domain partitioning with denser sampling in harder-to-approximate areas. Furthermore, upper-bounding the number of samples for each sub-domain enforces an upper bound on the condition number of the covariance matrices, leading to numerically reliable computations, even for millions of samples, without requiring any regularization (P4).

B. Proposed algorithm

We partition the domain \mathcal{X} into sub-domains \mathcal{X}_a , i.e., $\mathcal{X} = \cup_{a \in \mathcal{A}} \mathcal{X}_a$, $\mathcal{A} \subseteq \mathbb{N}$, where each sub-domain is a cube. Each sub-domain \mathcal{X}_a has an individual length scale ℓ_a and an individually scaled kernel \tilde{k}_a with

$$\tilde{k}_a(\cdot) := \tilde{k} \left(\frac{\cdot}{\ell_a} \right), \quad \ell_a = \max_{x_i, x_j \in \mathcal{X}_a} \|x_i - x_j\|_\infty. \quad (10)$$

Accordingly, the covariance matrix, the covariance vector, and the function \mathfrak{K} (see (9)) for each sub-domain $a \in \mathcal{A}$ are denoted by $K_{a,X}$, $k_{a,X}$, and \mathfrak{K}_a , respectively.

We sample equidistantly in every sub-domain \mathcal{X}_a with grid size $\Delta x_a > 0$, which is chosen such that $\ell_a / \Delta x_a = 2^{p_a}$ with some later specified $p_a \in \mathbb{N}_{\geq \underline{p}}$ and a user-chosen hyperparameter $\underline{p} > 0$. For any $p \geq \underline{p}$, we denote by $X_{a,p}$ the set of $(1 + 2^p)^n$ equidistant samples on sub-domain \mathcal{X}_a . The total samples on the domain \mathcal{X} are thus given by $X = \cup_{a \in \mathcal{A}} X_{a,p_a}$.

Additionally, we divide the sub-domain \mathcal{X}_a into uniform local cubes \mathcal{X}_c , i.e., $\mathcal{X}_a = \cup_{c \in \mathcal{C}_{a,p_a}} \mathcal{X}_c$, $\mathcal{C}_{a,p_a} \subseteq \mathbb{N}$, of edge length Δx_a . Each local cube \mathcal{X}_c has 2^n samples on its vertices, which we denote by X_c . The center \bar{x}_c of local cube \mathcal{X}_c is given by $\bar{x}_c = \frac{1}{2^n} \sum_{x \in X_c} x$. The samples on sub-domain $\mathcal{X}_a \supseteq \mathcal{X}_c$ can be obtained with $X_{a,p_a} = \cup_{c \in \mathcal{C}_{a,p_a}} X_c$.

The resulting structure is shown in Figure 3. For each local cube \mathcal{X}_c , we define a localized approximating function h_{X_c} that only depends on the 2^n samples X_c , leading to a piecewise-defined approximating function and a localized kernel interpolation approach.

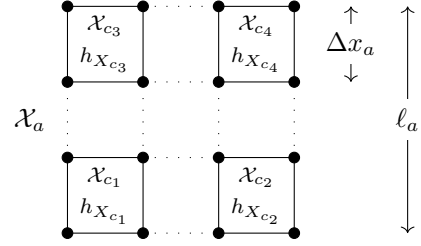


Fig. 3. Structure of the resulting uniform local cubes and the localized approximating functions on a sub-domain \mathcal{X}_a with length scale ℓ_a and grid size Δx_a . Illustrated are the local cubes \mathcal{X}_c , $c \in \{c_1, c_2, c_3, c_4\} \subseteq \mathcal{C}_{a,p_a}$.

For the approximation procedure, we use function values that are shifted by an empirical mean value, i.e.,

$$\tilde{f}_{X_{a,p}} = f_{X_{a,p}} - \mu_a, \quad \mu_a := \frac{\sum_{x \in X_{a,p}} f(x)}{\text{card}(X_{a,p})}. \quad (11)$$

Due to the continuity of the ground truth (see Lemma 1), this shifting ensures arbitrarily small function values $\tilde{f}_{X_{a,p}}$ for decreasing size of the sub-domain \mathcal{X}_a , which later assists in guaranteeing an arbitrarily small approximation error $\epsilon > 0$. For any local cube $\mathcal{X}_c \subseteq \mathcal{X}_a$ with samples $X_c \subseteq X_{a,p_a}$, the localized kernel interpolation with shifted function values (11) results in the shifted localized approximating function (see (4))

$$\tilde{h}_{X_c}(x) = \tilde{f}_{X_c}^\top K_{a,X_c}^{-1} \tilde{k}_{a,X_c}(x). \quad (12)$$

To construct the shifted localized approximating functions on a sub-domain \mathcal{X}_a , we first query the ground truth at the inputs X_{a,p_a} and shift the samples by the empirical mean μ_a . With these samples, we compute the shifted localized approximating functions (12) for all local cubes $\mathcal{X}_c \subseteq \mathcal{X}_a$. Algorithm 1 summarizes this procedure.

Algorithm 1 Shifted localized approximating functions

Require: f , \tilde{k}_a , X_{a,p_a}

- 1: Sample $f_{X_{a,p_a}}$ ▷ (2)
 - 2: Compute mean μ_a and shifted values $\tilde{f}_{X_{a,p_a}}$ ▷ (11)
 - 3: Define cube partition \mathcal{C}_{a,p_a} from X_{a,p_a}
 - 4: **for** $c \in \mathcal{C}_{a,p_a}$ **do**
 - 5: Build approximating function \tilde{h}_{X_c} ▷ (12)
-

In the following, we ensure that the shifted localized approximating functions computed in Algorithm 1 satisfy the desired error bound ϵ . First, we define the shifted ground truth \tilde{f}_a on sub-domain \mathcal{X}_a as

$$\tilde{f}_a(x) := f(x) - \mu_a. \quad (13)$$

Given the sub-domain partitioning and the local approximation scheme, the desired approximation error bound (1) reduces to

$$|\tilde{f}_a(x) - \tilde{h}_{X_c}(x)| \leq \epsilon \quad \forall a \in \mathcal{A}, \forall c \in \mathcal{C}_{a,p_a}, \forall x \in \mathcal{X}_c. \quad (14)$$

Furthermore, analogous to standard kernel-based approximation methods (see e.g., [29], [30], [38]–[43]), we require knowledge of an upper bound on the corresponding RKHS norm.

Assumption 3. For any $a \in \mathcal{A}$, \tilde{f}_a is a member of the RHKS of kernel \tilde{k}_a . Moreover, we have access to an oracle $\bar{\Gamma}_a \in (0, \infty)$, which is an upper bound on the RHKS norm, i.e., $\bar{\Gamma}_a \geq \|\tilde{f}_a\|_{\tilde{k}_a}$.

In Section IV, we introduce a heuristic approximation that replaces the oracle assumption.

The following result provides a lower bound on the number of samples that ensure the desired error bound ϵ for each sub-domain \mathcal{X}_a .

Proposition 2. Let Assumptions 1–3 hold. For any $a \in \mathcal{A}$ and any $\epsilon > 0$, there exists a $p_a^* \in \mathbb{N}$ such that $p_a \geq p_a^*$ implies $P_{X_c}(\bar{x}_c)\bar{\Gamma}_a \leq \epsilon$ for all $c \in \mathcal{C}_{a,p_a}$. Furthermore, if $p_a \geq p_a^*$ for all $a \in \mathcal{A}$, then the localized approximating functions according to Algorithm 1 satisfy (14).

Proof. The proof is divided into three parts. In Part I, we bound the power function $P_{X_c}(\bar{x}_c)$ using an eigenvector of the covariance matrix. In Part II, we show that $P_{X_c}(\bar{x}_c)\bar{\Gamma}_a \leq \epsilon$ holds for $p_a \geq p_a^*$, while in Part III we prove that this implies (14).

Part I: Pick any $a \in \mathcal{A}$. For any $c \in \mathcal{C}_{a,p_a}$, given samples X_c on the vertices of local cube \mathcal{X}_c , we denote the scaled covariance matrix and the scaled covariance vector by K_{a,X_c} and k_{a,X_c} , respectively. In this cubic setting, the covariance matrix K_{a,X_c} has constant row sum. Moreover, the covariance vector satisfies $k_{a,X_c}(\bar{x}_c) = \tilde{k}_a\left(\frac{\sqrt{n}\Delta x_a}{2}\right) \cdot \mathbf{1}_{2^n}$. Therefore, $k_{a,X_c}(\bar{x}_c)$ is an eigenvector of K_{a,X_c} with eigenvalue

$$\beta = \sum_{x \in X_c} \tilde{k}_a(\|x - x'\|_2) \stackrel{\text{Asm.1}}{\leq} 2^n \quad (15)$$

for an arbitrary $x' \in X_c$. Hence, we have

$$K_{a,X_c}^{-1} k_{a,X_c}(\bar{x}_c) = \frac{1}{\beta} k_{a,X_c}(\bar{x}_c). \quad (16)$$

This yields

$$\begin{aligned} P_{X_c}(\bar{x}_c) &\stackrel{(6),(16)}{\leq} \sqrt{1 - \frac{\tilde{k}_a\left(\frac{\sqrt{n}\Delta x_a}{2}\right)^2 2^n}{\beta}} \\ &\stackrel{(15)}{\leq} \sqrt{1 - \tilde{k}_a\left(\frac{\sqrt{n}\Delta x_a}{2}\right)^2}. \end{aligned} \quad (17)$$

Part II: We introduce the notation $\lceil \xi \rceil \in \mathbb{N}$ as rounding $\xi \in \mathbb{R}$ up to the nearest integer. First, suppose $\epsilon < \bar{\Gamma}_a$ and define

$$p_a^* := \left\lceil \log_2 \left(\frac{\ell_a \sqrt{n}}{2\mathfrak{K}_a^{-1}\left(\frac{1}{2}\left(\frac{\epsilon}{\bar{\Gamma}_a}\right)^2\right)} \right) \right\rceil. \quad (18)$$

For any $p_a \geq p_a^*$, any $c \in \mathcal{C}_{a,p_a}$, and any $\epsilon > 0$, it holds that

$$\begin{aligned} P_{X_c}(\bar{x}_c)\bar{\Gamma}_a &\stackrel{(17)}{\leq} \bar{\Gamma}_a \sqrt{1 - \tilde{k}_a\left(\frac{\sqrt{n}\Delta x_a}{2}\right)^2} \\ &= \bar{\Gamma}_a \sqrt{\left(1 - \tilde{k}_a\left(\frac{\sqrt{n}\Delta x_a}{2}\right)\right) \left(1 + \tilde{k}_a\left(\frac{\sqrt{n}\Delta x_a}{2}\right)\right)} \end{aligned}$$

$$\begin{aligned} &\stackrel{(9)}{=} \bar{\Gamma}_a \sqrt{\mathfrak{K}_a\left(\frac{\sqrt{n}\Delta x_a}{2}\right) \left(1 + \tilde{k}_a\left(\frac{\sqrt{n}\Delta x_a}{2}\right)\right)} \\ &\leq \bar{\Gamma}_a \sqrt{2\mathfrak{K}_a\left(\frac{\sqrt{n}\Delta x_a}{2}\right)} = \bar{\Gamma}_a \sqrt{2\mathfrak{K}_a\left(\frac{\sqrt{n}\ell_a}{2 \cdot 2^{p_a}}\right)} \\ &\stackrel{(18)}{\leq} \bar{\Gamma}_a \sqrt{2\mathfrak{K}_a\left(\mathfrak{K}_a^{-1}\left(\frac{1}{2}\left(\frac{\epsilon}{\bar{\Gamma}_a}\right)^2\right)\right)} = \epsilon. \end{aligned} \quad (19)$$

Note that we used $2^{p_a} = \ell_a/\Delta x_a$ and the fact that $\mathfrak{K}_a \in \mathcal{K}_\infty$ and $\tilde{k}_a: \mathbb{R}_{\geq 0} \rightarrow (0, 1]$. In case of $\epsilon \geq \bar{\Gamma}_a$, $P_{X_c}(\bar{x}_c)\bar{\Gamma}_a \leq \epsilon$ (see (19)) holds for any $\Delta x_a > 0$ since $P_{X_c}(\bar{x}_c) \leq 1$ for all $p_a \geq p_a^* = 0$.

Part III: For any $c \in \mathcal{C}_{a,p_a}$ and for any $x \in \mathcal{X}_c$, given the sub-domain partitioning and the local approximation scheme, error bound (7) of Proposition 1 yields

$$|\tilde{f}_a(x) - \tilde{h}_{X_c}(x)| \leq P_{X_c}(x) \|\tilde{f}_a\|_{\tilde{k}_a}. \quad (20)$$

Thus, for any $p_a \geq p_a^*$, any $c \in \mathcal{C}_{a,p_a}$, any $x \in \mathcal{X}_c$, and any $\epsilon > 0$, it holds that

$$\begin{aligned} |\tilde{f}_a(x) - \tilde{h}_{X_c}(x)| &\stackrel{(20)}{\leq} P_{X_c}(x) \|\tilde{f}_a\|_{\tilde{k}_a} \stackrel{\text{Asm.2}}{\leq} P_{X_c}(\bar{x}_c) \|\tilde{f}_a\|_{\tilde{k}_a} \\ &\stackrel{\text{Asm.3}}{\leq} P_{X_c}(\bar{x}_c)\bar{\Gamma}_a \leq \epsilon, \end{aligned}$$

where the last inequality was shown in Part II. \square

Proposition 2 ensures arbitrary approximation accuracy ϵ using a local approximation scheme by sampling densely enough. Since we additionally enforce a lower bound $p_a \geq \underline{p}$, we choose

$$p_a = \max\{\underline{p}, p_a^*\}. \quad (21)$$

For small accuracies ϵ , this may result in large values p_a , which deteriorates the conditioning of the covariance matrices K_{a,X_c} , resulting in numerical unreliability. Thus, we introduce $\bar{p} > \underline{p}$, an upper bound on the integer p_a . This yields a uniform upper bound $\bar{\kappa}$ on the condition number

$$\text{cond}(K_{a,X_c}) \leq \bar{\kappa} \quad \forall a \in \mathcal{A}, \forall p \in \{\underline{p}, \dots, \bar{p}\}, \forall c \in \mathcal{C}_{a,p}, \quad (22)$$

with $\text{cond}(K_{a,X_c}) := \|K_{a,X_c}\|_\infty \|K_{a,X_c}^{-1}\|_\infty$. For a given $p_a \geq \underline{p}$, we have a fixed ratio $\ell_a/\Delta x_a = 2^{p_a}$, and hence K_{a,X_c} is identical for any $c \in \mathcal{C}_{a,p_a}$ and any $a \in \mathcal{A}$. Thus, given a uniformly bounded $p_a \in \{\underline{p}, \dots, \bar{p}\}$, this yields a uniform bound on the condition number $\bar{\kappa}$. Furthermore, \bar{p} and $\bar{\kappa}$ have one-to-one correspondence.³ If (21) returns $p_a > \bar{p}$, we partition the sub-domain \mathcal{X}_a into 2^n cubes of the same size, which halves the length scale ℓ_a , allowing for a denser sampling.

The overall offline approximation is summarized in Algorithm 2. To compute a sufficiently accurate approximation of the ground truth f on the domain \mathcal{X} , we iterate through a dynamic for-loop to determine the localized approximating

³In fact, (22) can be enforced a priori. First, we define $\mathcal{C}_{\bar{p}}$ as the cube partition resulting from $\text{card}(X) = (1 + 2^{\bar{p}})^n$ equidistant samples on the domain $\mathcal{X} = [0, 1]^n$. Then, we compute the covariance matrix of the unscaled kernel k (i.e., with $\ell = 1$) for an arbitrary $c \in \mathcal{C}_{\bar{p}}$ with 2^n samples X_c and check whether $\text{cond}(K_{X_c}) \leq \bar{\kappa}$.

functions for all sub-domains. After querying the oracle to receive an upper bound on the RKHS norm of the ground truth $\bar{\Gamma}_a$, we determine the number of samples for the current sub-domain with (21). If $p_a \leq \bar{p}$, then the matrices are well-conditioned according to (22) and we define the localized approximating functions for the current sub-domain. If $p_a > \bar{p}$, we partition \mathcal{X}_a further into 2^n uniform sub-domains. We continue with the described procedure until we have constructed localized approximating functions that cover the whole domain.

Algorithm 2 Adaptive and Localized Kernel Interpolation

Require: $f, \mathcal{X}, \tilde{k}, \epsilon, \underline{p}, \bar{p}$

- 1: Init: $\mathcal{A} = \{0\}, \mathcal{X}_0 = \mathcal{X}$
- 2: **for** $a \in \mathcal{A}$ **do** ▷ Dynamic for-loop
- 3: Query oracle for $\bar{\Gamma}_a$ ▷ Asm. 3
- 4: Determine sufficiently large p_a ▷ Prop. 2, (21)
- 5: **if** $p_a \leq \bar{p}$ **then** ▷ (22)
- 6: Get localized approximating functions ▷ Alg. 1
- 7: **else**
- 8: Define 2^n new sub-domains $\cup_{a' \in \mathcal{A}'} \mathcal{X}_{a'} = \mathcal{X}_a$
- 9: $\mathcal{A} \leftarrow \mathcal{A} \cup \mathcal{A}' \setminus a$ ▷ Update set partitions

The resulting localized approximating functions are used for the online evaluation, which is described in Algorithm 3. First, we define the function $h: \mathcal{X} \rightarrow \mathbb{R}$ as the piecewise-defined approximating function on the domain \mathcal{X} , i.e., for any $a \in \mathcal{A}$, $c \in \mathcal{C}_{a,p_a}$, and $x \in \mathcal{X}_c$, we define

$$\tilde{h}(x) := \tilde{h}_{X_c}(x), \quad h(x) := \tilde{h}_{X_c}(x) + \mu_a. \quad (23)$$

For the online evaluation, we determine the relevant local cube \mathcal{X}_c such that $x \in \mathcal{X}_c$ by performing a tree search, and then evaluate the localized approximating function, similar to the online evaluation in [36].

Algorithm 3 Online Evaluation

Require: \tilde{h}, x

- 1: Tree search $c \in \mathcal{C}_{a,p_a}, a \in \mathcal{A}$ such that $x \in \mathcal{X}_c \subseteq \mathcal{X}_a \subseteq \mathcal{X}$
- 2: **return** $h(x)$

C. Sample complexity and uniform approximation error

To derive an upper bound on the maximum number of samples, we use the following assumption on the ground truth.

Assumption 4. *There exists a function $\alpha \in \mathcal{K}_\infty$ such that for any $a \in \mathcal{A}$, the oracle in Assumption 3 satisfies*

$$\alpha(\bar{\Gamma}_a) \leq \ell_a. \quad (24)$$

Shifted function values in combination with a continuous ground truth (see Lemma 1) ensure $\lim_{\ell_a \rightarrow 0} \tilde{f}_a(x) = 0$ for all $x \in \mathcal{X}_a$, which implies $\lim_{\ell_a \rightarrow 0} \|\tilde{f}_a\|_{\tilde{k}_a} = 0$, and hence provides an intuition for Assumption 4. In fact, in the proof of Theorem 2, we show that the RKHS norm of the approximating function is upper-bounded by $\alpha^{-1}(\ell_a)$ with some later specified $\alpha \in \mathcal{K}_\infty$.

The following theorem provides an upper bound on the sample complexity (P3) and ensures that the localized approximating functions satisfy error bound ϵ (P2).

Theorem 1. *Let Assumptions 1–4 hold. Then, Algorithm 2 terminates after querying at most $\text{card}(X) \leq \mathcal{O}((1/\alpha(\epsilon))^n)$ samples. Furthermore, the resulting approximating function (Alg. 3) satisfies Inequality (1), i.e., the approximation error is uniformly bounded by $\epsilon > 0$.*

Proof. The proof is divided into three parts. In Part I, we show that Algorithm 2 terminates once a threshold length scale is reached. In Part II, we derive the worst-case sample complexity in order to reach this threshold length scale. In Part III, we demonstrate that the resulting localized approximating functions satisfy error bound ϵ .

Part I: Consider any $a \in \mathcal{A}$. First, we show that Algorithm 2 terminates whenever

$$\ell_a \leq \alpha(\epsilon). \quad (25)$$

For any $c \in \mathcal{C}_{a,p_a}$, it holds that

$$\bar{\Gamma}_a \stackrel{(24)}{\leq} \alpha^{-1}(\ell_a) \stackrel{(25)}{\leq} \alpha^{-1}(\alpha(\epsilon)) = \epsilon, \quad (26)$$

which yields $p_a^* = 0$ in Proposition 2. Therefore, (21) returns $p_a = \underline{p} \leq \bar{p}$, i.e., Algorithm 2 terminates if (25) is satisfied. Thus, since the length scale ℓ_a is halved with each partitioning,

$$\ell_a > \frac{\alpha(\epsilon)}{2} \quad (27)$$

always holds for any partition $a \in \mathcal{A}$.

Part II: The number of sub-domains satisfies

$$\text{card}(\mathcal{A}) \leq \left(\min_{a \in \mathcal{A}} \ell_a \right)^{-n} \stackrel{(27)}{<} \left(\frac{2}{\alpha(\epsilon)} \right)^n. \quad (28)$$

Moreover, each sub-domain \mathcal{X}_a has at most

$$\text{card}(X_a) \stackrel{(22)}{\leq} (1 + 2^{\bar{p}})^n \quad (29)$$

samples. Thus, Algorithm 2 terminates after at most

$$\begin{aligned} \text{card}(X) &= \sum_{a \in \mathcal{A}} \text{card}(X_a) \stackrel{(28),(29)}{<} \left(\frac{2}{\alpha(\epsilon)} \right)^n (1 + 2^{\bar{p}})^n \\ &= \mathcal{O} \left(\left(\frac{1}{\alpha(\epsilon)} \right)^n \right) \end{aligned}$$

samples.

Part III: Once Algorithm 2 has terminated, each sub-domain \mathcal{X}_a satisfies $p_a \geq p_a^*$. Hence, Proposition 2 ensures the satisfaction of error bound (14). For any $c \in \mathcal{C}_{a,p_a}$, any $a \in \mathcal{A}$, and any $x \in \mathcal{X}_c$, we have that $|f(x) - h(x)| \stackrel{(13),(23)}{=} |\tilde{f}_a(x) - \tilde{h}_{X_c}(x)| \stackrel{(14)}{\leq} \epsilon$, i.e., error bound (1) holds. \square

The approach proposed in this section leads to a one-shot algorithm with explicit worst-case sample complexity and a guaranteed error bound. However, assuming a known RKHS norm of the unknown ground truth (see Assumptions 3 and 4) can be restrictive in practice. In the next section, we alleviate this issue by introducing a heuristic.

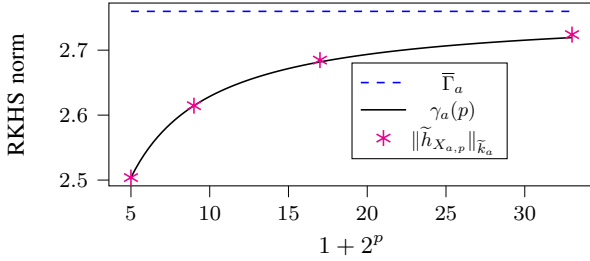


Fig. 4. Illustration of the RKHS norm extrapolation. The magenta asterisks show the RKHS norm of the approximating function $\|\tilde{h}_{X_{a,p}}\|_{\tilde{k}_a}$ (30). The solid black line is the extrapolating function γ_a (33), while the dashed blue line depicts its limit value $\bar{\Gamma}_a$ (35).

IV. ALKIA-X

In this section, we extend the algorithm proposed in Section III to unknown RKHS norms by introducing a heuristic RKHS norm extrapolation. This extension yields ALKIA-X, the Adaptive and Localized Kernel Interpolation Algorithm with eXtrapolated RKHS norm. In Section IV-A, we introduce the main idea before explaining the details of the RKHS norm extrapolation in Section IV-B. We provide the theoretical analysis in Section IV-C, including the guaranteed error bound and the worst-case sample complexity. Then, we present simpler complexity bounds for a popular kernel choice in Section IV-D.

A. Main idea

ALKIA-X has one major difference compared to the algorithm presented in Section III: instead of assuming access to an oracle that returns an upper bound on the RKHS norm of the unknown ground truth (see Assumption 3), we introduce a novel *RKHS norm extrapolation* (T3). Specifically, we follow an extrapolation from the RKHS norm of the approximating function for each sub-domain \mathcal{X}_a . Figure 4 shows that the trend of the RKHS norm of the approximating function empirically resembles exponential behavior.⁴ Hence, we fit an *exponential* function to the first two values of the RKHS norm of the approximating function and assume that its limit provides an upper bound on the RKHS norm of the unknown ground truth for each sub-domain.

B. RKHS norm extrapolation

In the following, we formalize the exponential extrapolating function. To this end, we first introduce the RKHS norm of the shifted approximating function of sub-domain \mathcal{X}_a based on $\text{card}(X_{a,\hat{p}}) = (1 + 2^{\hat{p}})^n$ samples as

$$\|\tilde{h}_{X_{a,\hat{p}}}\|_{\tilde{k}_a} = \sqrt{\tilde{f}_{X_{a,\hat{p}}}^\top K_{a,X_{a,\hat{p}}}^{-1} \tilde{f}_{X_{a,\hat{p}}}} \quad \forall \hat{p} \in \{\underline{p}, \dots, \bar{p}\}. \quad (30)$$

Note that we only use $\|\tilde{h}_{X_{a,\hat{p}}}\|_{\tilde{k}_a}$ for $\hat{p} \in \{\underline{p}, \underline{p}+1\}$ to construct the extrapolating function. To guarantee well-conditioned computations, we require that

$$\text{cond}(K_{a,X_{a,\hat{p}}}) \leq \bar{\kappa} \quad \forall \hat{p} \in \{\underline{p}, \underline{p}+1\}, \forall a \in \mathcal{A} \quad (31)$$

⁴The results in Figure 4 are generated using the Matérn kernel [34] with $\nu = 3/2$ and the function $f: [0, 1]^2 \rightarrow \mathbb{R}$ with $f(x) = \sin(2\pi x_1) + \cos(2\pi x_2)$, where $x = [x_1, x_2]^\top \in \mathbb{R}^2$ and $\mathcal{X}_a = [0, 1/3]^2$. The remaining hyperparameters are $\underline{p} = 2$, $\bar{p} = 5$ ($\bar{\kappa} = 1.14 \cdot 10^8$), and $\epsilon = 10^{-6}$.

holds in addition to (22). Note that (31) is enforced through the choice of \underline{p} , and that \underline{p} and $\bar{\kappa}$ have one-to-one correspondence and are uniform bounds.⁵

We upper-bound $\|\tilde{h}_{X_{a,\hat{p}}}\|_{\tilde{k}_a}$, $\hat{p} \in \{\underline{p}, \underline{p}+1\}$ with

$$\hat{\gamma}_{a,\hat{p}} = \|\tilde{h}_{X_{a,\hat{p}}}\|_{\tilde{k}_a} + \frac{\epsilon}{2^{\lambda+1}}, \quad \lambda := 2 + 2^{-\underline{p}}. \quad (32)$$

The form of this upper bound becomes clearer when developing the theoretical guarantees in Section IV-C. The extrapolating function $\gamma_a: \mathbb{N}_{\geq \underline{p}} \rightarrow \mathbb{R}_{\geq 0}$ is given by

$$\gamma_a(p) := \bar{\Gamma}_a \exp\left(-\frac{\tau_a}{1 + 2^p}\right) \quad \forall p \in \{\underline{p}, \dots, \bar{p}\}, \quad (33)$$

where $\bar{\Gamma}_a$ is the limit of the extrapolating function and τ_a determines the rate at which the extrapolating function approaches its limit value.

Lemma 2. For any $a \in \mathcal{A}$ and any $\hat{p} \in \{\underline{p}, \underline{p}+1\}$, it holds that

$$\gamma_a(\hat{p}) = \hat{\gamma}_{a,\hat{p}} \quad (34)$$

with

$$\tau_a = \ln\left(\frac{\hat{\gamma}_{a,\underline{p}+1}}{\hat{\gamma}_{a,\underline{p}}}\right) \lambda (1 + 2^{\underline{p}}), \quad \bar{\Gamma}_a = \hat{\gamma}_{a,\underline{p}} \left(\frac{\hat{\gamma}_{a,\underline{p}+1}}{\hat{\gamma}_{a,\underline{p}}}\right)^\lambda \quad (35)$$

and $\bar{\Gamma}_a \in (0, \infty)$.

The proof can be found in Appendix B. Figure 4 depicts the RKHS norm extrapolation heuristic applied to a toy example. The resulting extrapolation approximates the trend of the RKHS norm of the approximating function well, although it has been constructed with the first two values $\|\tilde{h}_{X_{a,p}}\|_{\tilde{k}_a}$, $p \in \{\underline{p}, \underline{p}+1\}$ only. We use the limit of the extrapolating function $\bar{\Gamma}_a$ as an upper bound on the RKHS norm, which we formalize in Assumption 5.

Assumption 5. For any $a \in \mathcal{A}$, \tilde{f}_a is a member of the RKHS of kernel \tilde{k}_a . Moreover, the limit of the extrapolating function $\bar{\Gamma}_a \in (0, \infty)$ (see (33), (35)) is an upper bound on the RKHS norm, i.e., $\bar{\Gamma}_a \geq \|\tilde{f}_a\|_{\tilde{k}_a}$.

Remark 1. (RKHS norm approximation) In general, it is not possible to find an upper bound on the RKHS norm of the ground truth $\|f\|_k$ (or any shifted or restricted version of it) from finite samples, since it is an underlying characteristic of an unknown function. Thus, there exists no perfect solution to tackle the challenging problem of working with the RKHS norm of an unknown ground truth. A basic approach, followed by many related works (see e.g., [29], [30], [38]–[43]) and also in Section III of this paper, is to assume that an oracle is available that returns a not overly conservative upper bound on the RKHS norm. In order to not rely on an oracle, we introduce the RKHS norm extrapolation (33) with its

⁵Akin to (22), for a fixed $\underline{p} > 0$, the condition number $\text{cond}(K_{a,X_{a,\underline{p}+1}})$ is identical for each sub-domain \mathcal{X}_a . Moreover, (31) can be enforced a priori by checking whether the covariance matrix of the unscaled kernel k (i.e., with $\ell = 1$) with $\text{card}(X) = (1 + 2^{\underline{p}+1})^n$ equidistant samples on domain $\mathcal{X} = [0, 1]^n$ is well-conditioned, i.e., whether $\text{cond}(K_X) \leq \bar{\kappa}$.

corresponding limit (35). The considered extrapolation is only a heuristic and Assumption 5 may fail on some occasions.

Some early works in the field of information theory and signal detection compute the RKHS norm of the ground truth function. However, the authors assume that an explicit expression of the ground truth is known [48], [49], which is not the case in the setting of this paper. Moreover, in [50], an upper bound on the RKHS norm of the ground truth based on the RKHS norm of the approximating function is derived. However, the authors assume that the ground truth is a member of a pre-RKHS spanned by the chosen kernel (see e.g., [33, Section 2.3]), which is more restrictive.

In the following, we briefly mention other approximations of $\|f\|_k$ using $\|h_X\|_k$. As noted in [30, Remark 2], the RKHS norm of the approximating function $\|h_X\|_k$ is an underestimation of the RKHS norm of the ground truth $\|f\|_k$. In [29, Appendix A], the authors use the intuition that $\|h_X\|_k$ may converge to $\|f\|_k$ for an increasing sample set X . Based hereon, [43, Appendix A] estimates an upper bound by manually checking the convergence of $\|h_X\|_k$. In contrast, we provide a simple formula to automatically extrapolate an estimate of the RKHS norm, which improves the ideas presented in [29], [43] and empirically tends to closely match the underlying ground truth as seen in Figure 4.

The offline approximation using ALKIA-X is summarized in Algorithm 4. Compared to Algorithm 2 in Section III, instead of receiving an upper bound on the RKHS norm of the ground truth from an oracle (see Assumption 3), we use the exponential extrapolation to compute $\bar{\Gamma}_a$ (see Assumption 5). As a result, the exact number of required samples is determined during the approximation procedure, as $\bar{\Gamma}_a$ is not known a priori.

Algorithm 4 ALKIA-X

Require: $f, \mathcal{X}, \tilde{k}, \epsilon, \underline{p}, \bar{p}$ ▷ (31)
1: Init: $\mathcal{A} = \{0\}, \mathcal{X}_0 = \mathcal{X}$
2: **for** $a \in \mathcal{A}$ **do** ▷ Dynamic for-loop
3: Get samples $\tilde{f}_{X_{a,\hat{p}}}, \hat{p} \in \{\underline{p}, \underline{p} + 1\}$ ▷ (2), (11)
4: Compute $\bar{\Gamma}_a$ ▷ (30), (32), (35)
5: Determine sufficiently large p_a ▷ Prop. 2, (21)
6: **if** $p_a \leq \bar{p}$ **then** ▷ (22)
7: Get localized approximating function ▷ Alg. 1
8: **else**
9: Define 2^n new sub-domains $\cup_{a' \in \mathcal{A}'} \mathcal{X}_{a'} = \mathcal{X}_a$
10: $\mathcal{A} \leftarrow \mathcal{A} \cup \mathcal{A}' \setminus a$ ▷ Update set partitions

C. Sample complexity and uniform approximation error

The following theorem provides a bound on the sample complexity and ensures the satisfaction of error bound ϵ .

Theorem 2. *Let Assumptions 1, 2, and 5 hold. Then, Algorithm 4 terminates after at most*

$$\text{card}(X) \leq \mathcal{O} \left(\left(\frac{\sqrt{n}}{\mathfrak{K}^{-1} \left(C \left(\frac{\epsilon}{\|f\|_k} \right)^2 \right)} \right)^n \right) \quad (36)$$

samples, with some $C > 0$ independent of ϵ, f . Furthermore, the resulting approximating function (Alg. 3) satisfies Inequality (1), i.e., the approximation error is uniformly bounded by $\epsilon > 0$.

Proof. The proof is structured analogously to the proof of Theorem 1. In Part I, we show that Algorithm 4 terminates once a threshold length scale is reached. In Part II, we derive the worst-case sample complexity in order to reach that threshold length scale. In Part III, we demonstrate that the resulting localized approximating functions satisfy error bound ϵ .

Part I: Consider any $a \in \mathcal{A}$. First, we prove that $|\tilde{f}_a(x)| \leq \|f\|_k \sqrt{2\mathfrak{K}(\sqrt{n}\ell_a)}$ holds for all $x \in \mathcal{X}_a$. Consider an arbitrary $x \in \mathcal{X}_a$, where, w.l.o.g., $\tilde{f}_a(x) \geq 0$. Pick any other $x' \in \mathcal{X}_a$ with $\tilde{f}_a(x') \leq 0$, which exists since $\sum_{x \in \mathcal{X}_{a,\underline{p}}} \tilde{f}_a(x) = 0$ (see (11)). It holds that

$$\begin{aligned} |\tilde{f}_a(x)| &\leq |\tilde{f}_a(x) - \tilde{f}_a(x')| \stackrel{(13)}{=} |f(x) - f(x')| \quad (37) \\ &\stackrel{\text{Lem. 1}}{\leq} \|f\|_k \sqrt{2\mathfrak{K}(\|x - x'\|_2)} \stackrel{(10)}{\leq} \|f\|_k \sqrt{2\mathfrak{K}(\sqrt{n}\ell_a)}. \end{aligned}$$

Next, we derive an upper bound on $\|\tilde{h}_{X_{a,\hat{p}}}\|_{\tilde{k}_a}$. For all $\hat{p} \in \{\underline{p}, \underline{p} + 1\}$, it holds that

$$\begin{aligned} \|\tilde{h}_{X_{a,\hat{p}}}\|_{\tilde{k}_a} &\stackrel{(5)}{=} \sqrt{\tilde{f}_{X_{a,\hat{p}}}^\top K_{a,X_{a,\hat{p}}}^{-1} \tilde{f}_{X_{a,\hat{p}}}} \\ &\leq \sqrt{\|\tilde{f}_{X_{a,\hat{p}}}\|_1 \|\tilde{f}_{X_{a,\hat{p}}}\|_\infty \|K_{a,X_{a,\hat{p}}}^{-1}\|_\infty} \quad (38) \\ &\stackrel{(37)}{\leq} \|f\|_k \sqrt{2\mathfrak{K}(\sqrt{n}\ell_a)} (1 + 2^{2^{p+1}})^n \|K_{a,X_{a,\hat{p}}}^{-1}\|_\infty \\ &\stackrel{(31)}{\leq} \|f\|_k \sqrt{2\mathfrak{K}(\sqrt{n}\ell_a)} (1 + 2^{2^{p+1}})^n \bar{\kappa}. \end{aligned}$$

The first inequality follows from Hölder's inequality, whereas the second inequality holds since $\text{card}(X_{a,\hat{p}}) \leq (1 + 2^{2^{p+1}})^n$ for all $\hat{p} \in \{\underline{p}, \underline{p} + 1\}$. Moreover, the last inequality is satisfied since $\|K_{a,X_{a,\hat{p}}}^{-1}\|_\infty = \frac{\text{cond}(K_{a,X_{a,\hat{p}}})}{\|K_{a,X_{a,\hat{p}}}\|_\infty} \stackrel{(31)}{\leq} \bar{\kappa}$ with $\|K_{a,X_{a,\hat{p}}}\|_\infty \geq \max_{i,j} K_{a,X_{a,\hat{p}}}(i,j) = \tilde{k}(0) = 1$. In the following, we show that Algorithm 4 terminates whenever

$$\ell_a \leq \frac{\mathfrak{K}^{-1} \left(\frac{\epsilon^2}{2\bar{\kappa}(1+2^{2^{p+1}})^n 2^{2\lambda+2}} \|f\|_k^2 \right)}{\sqrt{n}}. \quad (39)$$

For any $\hat{p} \in \{\underline{p}, \underline{p} + 1\}$, (38) and (39) imply

$$\|\tilde{h}_{X_{a,\hat{p}}}\|_{\tilde{k}_a} \leq \frac{\epsilon}{2^{\lambda+1}}. \quad (40)$$

For any $c \in \mathcal{C}_{a,p_a}$, (40) implies

$$\begin{aligned} \bar{\Gamma}_a &\stackrel{(35)}{=} \hat{\gamma}_{a,\underline{p}} \left(\frac{\hat{\gamma}_{a,\underline{p}+1}}{\hat{\gamma}_{a,\underline{p}}} \right)^\lambda \\ &\stackrel{(32)}{=} \left(\|\tilde{h}_{X_{a,\underline{p}}}\|_{\tilde{k}_a} + \frac{\epsilon}{2^{\lambda+1}} \right) \left(\frac{\|\tilde{h}_{X_{a,\underline{p}+1}}\|_{\tilde{k}_a} + \frac{\epsilon}{2^{\lambda+1}}}{\|\tilde{h}_{X_{a,\underline{p}}}\|_{\tilde{k}_a} + \frac{\epsilon}{2^{\lambda+1}}} \right)^\lambda \quad (41) \\ &\leq \left(\|\tilde{h}_{X_{a,\underline{p}}}\|_{\tilde{k}_a} + \frac{\epsilon}{2^{\lambda+1}} \right) \left(\frac{\epsilon + \|\tilde{h}_{X_{a,\underline{p}+1}}\|_{\tilde{k}_a} 2^{\lambda+1}}{\epsilon} \right)^\lambda \\ &\stackrel{(40)}{\leq} \left(\frac{\epsilon}{2^{\lambda+1}} + \frac{\epsilon}{2^{\lambda+1}} \right) \left(\frac{\epsilon + \epsilon}{\epsilon} \right)^\lambda = \left(\frac{2\epsilon}{2^{\lambda+1}} \right) 2^\lambda = \epsilon. \end{aligned}$$

Thus, analogous to Part I of the proof of Theorem 1, this yields $p_a^* = 0$ in Proposition 2 and $p_a = \underline{p} \leq \bar{p}$ in (21), wherefore Algorithm 4 terminates if (39) is satisfied. Thus,

$$\ell_a > \frac{\mathfrak{K}^{-1} \left(\frac{\epsilon^2}{2\bar{\kappa}(1+2\bar{p})^n 2^{2\lambda+2} \|f\|_k^2} \right)}{2\sqrt{n}} \quad (42)$$

always holds. Hence, we have that

$$\ell_a \leq \mathcal{O} \left(\frac{\mathfrak{K}^{-1} \left(C \left(\frac{\epsilon}{\|f\|_k} \right)^2 \right)}{\sqrt{n}} \right) \quad \forall a \in \mathcal{A}, \quad (43)$$

where $C > 0$ is a constant that is independent of ϵ, f .

Part II: From Part II of the proof of Theorem 1, we know that $\text{card}(X) \leq (\min_{a \in \mathcal{A}} \ell_a)^{-n} (1 + 2\bar{p})^n$. With (43), it follows that

$$\begin{aligned} \text{card}(X) &\leq \mathcal{O} \left(\left(\frac{\sqrt{n}(1+2\bar{p})}{\mathfrak{K}^{-1} \left(C \left(\frac{\epsilon}{\|f\|_k} \right)^2 \right)} \right)^n \right) \\ &= \mathcal{O} \left(\left(\frac{\sqrt{n}}{\mathfrak{K}^{-1} \left(C \left(\frac{\epsilon}{\|f\|_k} \right)^2 \right)} \right)^n \right). \end{aligned} \quad (44)$$

Part III: The proof is analogous to Part III of the proof of Theorem 1. We determine $\bar{\Gamma}_a$ with Assumption 5 and receive p_a from Proposition 2 and (21). The satisfaction of Inequality (1) directly follows. \square

Since $\mathfrak{K}^{-1}(0) = 0$, we have that $\epsilon/\|f\|_k \rightarrow 0$ implies $\text{card}(X) \rightarrow \infty$. This result is intuitive, as more complex functions (corresponding to a larger RKHS norm $\|f\|_k$) or a smaller allowed approximation error ϵ require more samples. Furthermore, the theoretical results obtained in this section show that, in the worst case, the number of samples to terminate ALKIA-X may scale exponentially with the input dimension, which is expected and widely known as the curse of dimensionality.

D. Complexity bounds for the SE-kernel

In this section, we derive more intuitive bounds on the online and offline complexity for the special case of the squared-exponential (SE) kernel, which is one of the most common kernels. The following lemma provides a bound on the smallest length scale that can occur when executing Algorithm 4 (see Part II of the proof of Theorem 2).

Lemma 3. *Suppose that the assumptions in Theorem 2 hold and that k is the SE-kernel. Then, for any $a \in \mathcal{X}_a$, it holds that*

$$\ell_a \leq \mathcal{O} \left(\frac{\epsilon}{\sqrt{n}\|f\|_k} \right) \quad \text{as } \frac{\epsilon}{\|f\|_k} \rightarrow 0. \quad (45)$$

The proof can be found in Appendix C. Moreover, the following corollary provides an upper bound on the number of samples sufficient to terminate Algorithm 4.

Corollary 1. *Suppose that the conditions in Lemma 3 hold. Then, it holds that*

$$\text{card}(X) \leq \mathcal{O} \left(\left(\frac{\sqrt{n}\|f\|_k}{\epsilon} \right)^n \right) \quad \text{as } \frac{\epsilon}{\|f\|_k} \rightarrow 0. \quad (46)$$

Proof. From Part II of Theorem 1, we know that $\text{card}(X) \leq (\min_{a \in \mathcal{A}} \ell_a)^{-n} (1 + 2\bar{p})^n = \mathcal{O}((\min_{a \in \mathcal{A}} \ell_a)^{-n})$. For $\epsilon/\|f\|_k \rightarrow 0$, Equation (45) derived in Lemma 3 provides a bound on ℓ_a for all $a \in \mathcal{A}$, from which (46) directly follows. \square

Offline computational complexity: Inequality (46) shows that, for a given $\epsilon/\|f\|_k$, the number of maximum samples to terminate Algorithm 4 scales exponentially with the input dimension n . Since we store all samples X to generate the approximating functions (see Algorithm 1), the memory requirements also scale exponentially with n .

Online computational complexity: The online evaluation with Algorithm 3 for an input $x \in \mathcal{X}$ can be divided into three steps. First, we execute a tree search to find \mathcal{X}_c such that $x \in \mathcal{X}_c \subseteq \mathcal{X}_a \subseteq \mathcal{X}$. Second, we construct the covariance vector (3). Third, we evaluate the approximating function (12). Next, we elaborate on the complexity of each step.

Each sub-domain $\mathcal{X}_a \subseteq \mathcal{X}$ corresponds to a node of the resulting tree of the offline approximation. The domain \mathcal{X} corresponds to the root node and the sub-domains containing the local cubes with the localized approximating functions are located in the leaf nodes. The complexity of the tree search scales linearly with the depth of the tree. Since the length scale is halved from one depth level to the next one, the maximum depth $\bar{d} \in \mathbb{N}$ is given by

$$\bar{d} = \mathcal{O} \left(\log_2 \left(\left(\min_{a \in \mathcal{A}} \ell_a \right)^{-1} \right) \right) \stackrel{(45)}{\leq} \mathcal{O} \left(\log_2 \left(\frac{\|f\|_k \sqrt{n}}{\epsilon} \right) \right). \quad (47)$$

Hence, the computational complexity of the tree search only scales *logarithmically*. This result is comparable to the logarithmic complexity of localized GP regression obtained in [36].

Since we use local approximations based on local cubes with 2^n samples, each covariance vector (3) is 2^n -dimensional. Thus, to construct the covariance vector, the kernel needs to be evaluated at 2^n points.

In (12), the vector-matrix multiplication $f_{X_c}^\top K_{a, X_c}^{-1}$ can be computed offline, and hence evaluating the approximating function (12) online reduces to computing $2^n \times 2^n$ vector-vector multiplications.

To conclude, although the offline sample complexity and the memory requirements scale exponentially with the input dimension n for a given $\|f\|_k/\epsilon$, the online evaluation is characterized by operations of order 2^n that are *independent* of the desired accuracy ϵ and the ground truth f , and the tree search that scales *logarithmically* with $\|f\|_k \sqrt{n}/\epsilon$.

V. APPROXIMATE MPC VIA ALKIA-X

In this section, we investigate the characteristics of the approximate MPC obtained using ALKIA-X. As introduced in Section II-A, the ground truth f corresponds to the MPC feedback law $u = f(x)$ and ALKIA-X determines an explicit feedback law $u = h(x)$ that approximates the MPC feedback f on the domain \mathcal{X} .

Infeasible states: ALKIA-X requires a cubic domain \mathcal{X} and the evaluation of the ground truth f for any $x \in \mathcal{X}$. The set \mathcal{X} should represent the state constraints, and in the standard case of box constraints, they can be shifted and scaled to yield a cubic set \mathcal{X} . The evaluation of f requires the solution of the underlying NLP, which is only defined on some feasible set $\mathcal{X}_{\text{feas}}^f \subseteq \mathcal{X}$. We define function evaluations for infeasible states $x \in \mathcal{X} \setminus \mathcal{X}_{\text{feas}}^f$ by relaxing hard state and terminal constraints in the MPC formulation using slack variables and penalties [51]. Then, under suitable regularity conditions, the optimization problem returns the same solution as the original MPC for all feasible states $x \in \mathcal{X}_{\text{feas}}^f$ (see [52]), while also providing a well-defined solution for $x \in \mathcal{X} \setminus \mathcal{X}_{\text{feas}}^f$.

Feasible domain of the approximate MPC: Although we can obtain function evaluations for the whole domain \mathcal{X} during the offline approximation, there is no need for approximating the MPC on infeasible parts of the domain \mathcal{X} . If each state within a sub-domain results in a non-zero slack variable, ALKIA-X classifies that sub-domain as infeasible and does not continue the approximation process on that sub-domain. Hence, ALKIA-X defines its own feasible domain $\mathcal{X}_{\text{feas}}^h$ on which it computes an approximating function with the desired approximation accuracy ϵ . We assume that $\mathcal{X}_{\text{feas}}^f \subseteq \mathcal{X}_{\text{feas}}^h$ holds to ensure that the error bound ϵ is enforced for all feasible states $x \in \mathcal{X}_{\text{feas}}^f$.

Non-scalar ground truths: In Sections III and IV, we developed ALKIA-X with its corresponding guarantees for a scalar ground truth $f: \mathcal{X} \rightarrow \mathbb{R}$. However, as discussed in Section II-A, the MPC feedback law $f: \mathcal{X} \rightarrow \mathbb{R}^{n_u}$ is in general non-scalar, i.e., $n_u > 1$. We can approximate such non-scalar functions by treating each dimension separately. Specifically, in Algorithm 4, we determine the sufficiently large integer p_a corresponding to the sufficient number of samples as the maximum of the sufficient number of samples required to approximate each control input dimension separately. Moreover, the localized approximating functions for each dimension are constructed (see Algorithm 1) and evaluated (see Algorithm 3) independently. Hence, ALKIA-X ensures $\|f(x) - h(x)\|_\infty \leq \epsilon$ for all $x \in \mathcal{X}_{\text{feas}}^f \subseteq \mathcal{X}_{\text{feas}}^h$.

Closed-loop guarantees: We provide closed-loop guarantees on the approximate MPC by combining a robust MPC design with the guaranteed approximation error (see Figure 1). To this end, consider a disturbance set $\mathcal{W} \subseteq \mathbb{R}^n$ that upper-bounds the effect of inexactly approximating the control input, i.e., $\mathcal{W} \supseteq \{g(x, \tilde{u}) - g(x, u) \mid x \in \mathcal{X}, u \in \mathcal{U}, \|u - \tilde{u}\|_\infty \leq \epsilon\}$, see e.g., constructions in [8], [9].

Corollary 2. *Let f be according to the robust MPC design in [21, Problem (30)] with disturbance bound \mathcal{W} and suppose that the conditions in [21, Theorem 2] regarding $f, g, \mathcal{X}, \mathcal{U}, \mathcal{W}$ hold.⁶ Suppose further that the conditions in Theorem 2 hold and that h is constructed according to Algorithm 4, where we approximate each dimension independently. Then, for any*

⁶As discussed above, f is the robust MPC design with constraints relaxed using penalties to ensure that the function is defined for all $x \in \mathcal{X}$. We assume that the conditions in [52] hold, ensuring that $f(x)$ coincides with the minimizer of [21, Problem (30)] for all $x \in \mathcal{X}_{\text{feas}}^f$.

initial condition $x_0 \in \mathcal{X}_{\text{feas}}^f$, the closed-loop system $x_{t+1} = g(x_t, u_t)$, $u_t = h(x_t)$ ensures

- (i) *recursive feasibility $x_t \in \mathcal{X}_{\text{feas}}^f \subseteq \mathcal{X}_{\text{feas}}^h, \forall t \in \mathbb{N}$,*
- (ii) *constraint satisfaction $x_t \in \mathcal{X}, u_t \in \mathcal{U}, \forall t \in \mathbb{N}$,*
- (iii) *and practical⁷ asymptotic stability of $x = x_s$.*

Proof. Theorem 2 ensures that each dimension of the approximating function h , which we receive independently from Algorithm 4, satisfies Inequality (1), i.e., the satisfaction of $\|f(x) - h(x)\|_\infty \leq \epsilon$ is ensured for all $x \in \mathcal{X}_{\text{feas}}^h$. Hence, the closed-loop system satisfies $x_{t+1} = g(x_t, h(x_t)) =: g(x_t, f(x_t)) + w_t$ with $w_t \in \mathcal{W}$ for all $x \in \mathcal{X}_{\text{feas}}^f \subseteq \mathcal{X}_{\text{feas}}^h$. Thus, the closed-loop guarantees in [21, Theorem 2] with respect to disturbances $w_t \in \mathcal{W}$ apply. \square

These theoretical guarantees are equally applicable if any other nonlinear MPC scheme is approximated that is designed to be robust with respect to disturbances $w_t \in \mathcal{W}$, see e.g., [20]–[23] for corresponding designs.

Computational complexity: In the complexity analysis in Section IV-D, we showed that the offline computational complexity of ALKIA-X scales exponentially with the number of states n . In contrast, the computational complexity of classical explicit MPC approaches scales with the number of states, the number of constraints, and the prediction horizon [25, Section 3]. Hence, a major benefit of approximating MPC schemes using ALKIA-X is the fact that the computational complexity does *not* directly increase with the prediction horizon or the number of constraints used in the MPC formulation. Moreover, the online computational complexity of classical kernel-based methods scales cubically in the number of samples [34, Section 2.3]. In contrast, the online computational complexity of ALKIA-X only scales *logarithmically* with $\|f\|_k \sqrt{n}/\epsilon$. Thus, the resulting approximate MPC is fast-to-evaluate, and hence suitable to control nonlinear systems that require high sampling rates with relatively cheap hardware (P1).

VI. NUMERICAL EXPERIMENTS

In this section, we approximate two nonlinear MPC schemes using ALKIA-X. In Section VI-A, we apply ALKIA-X on an academic example and compare its performance with existing work. In Section VI-B, we demonstrate the practicability of ALKIA-X by approximating an MPC corresponding to a real-world application for which fast sampling rates are required and computational capacity is limited. ALKIA-X and both MPCs are implemented in Python. The MPC schemes are formulated using CasADi [53] and the underlying NLPs are solved with IPOPT [54] using just-in-time compilation. We conducted the offline approximations on a Linux server with 32 GB RAM parallelized on 8 cores. The online evaluation was performed using an Ubuntu laptop with 32 GB RAM and an Intel Core i7-12700H processor. Moreover, we used the Matérn kernel with $\nu = 3/2$ and a length scale of 0.8 for both experiments.

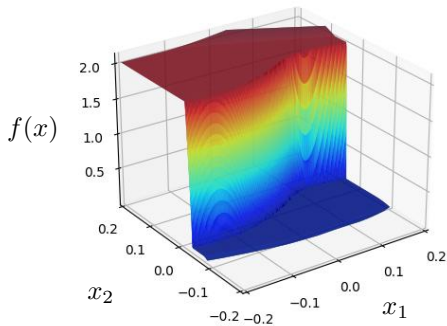


Fig. 5. Ground truth MPC feedback law f over the domain $\mathcal{X} = [-0.2, 0.2]^2$.

A. Continuous stirred tank reactor

We consider a nonlinear continuous stirred tank reactor with

$$g(x, u) = \begin{pmatrix} x_1 + \delta \left(\frac{1-x_1}{\theta} - \hat{k}x_1 e^{-\frac{M}{x_1}} \right) \\ x_2 + \delta \left(\frac{x_f - x_2}{\theta} + \hat{k}x_1 e^{-\frac{M}{x_2}} - \hat{c}u(x_2 - x_c) \right) \end{pmatrix}, \quad (48)$$

where x_1 is the temperature, x_2 is the concentration, u is the coolant flow, and $\delta = 0.1$ s is the sampling time, see [8] for details. The nonlinear MPC is formulated with a horizon of $N = 180$, the input constraint is $\mathcal{U} = [0, 2]$, and we obtain a cubic domain $\mathcal{X} = [-0.2, 0.2]^2$ after shifting, as done in [8].⁸ Figure 5 shows the corresponding MPC feedback law f over the domain $\mathcal{X} = [-0.2, 0.2]^2$.

We use ALKIA-X to determine an approximate MPC to control system (48) with high sampling rates and closed-loop guarantees. To this end, we consider the MPC scheme in [8], which is designed to be robust with respect to input disturbances bounded by $\epsilon = 5.1 \cdot 10^{-3}$. To compute the approximate MPC, ALKIA-X requires samples, i.e., solutions of the NLP of the ground truth MPC f for different states. In this experiment, the hyperparameters were $\underline{p} = 2$ and $\bar{p} = 5$, yielding an upper bound on the condition number of $\bar{\kappa} = 1.14 \cdot 10^8$ (see (22), (31)).

Result: We approximate the ground truth MPC feedback law f using ALKIA-X with the error bound $\epsilon = 5.1 \cdot 10^{-3}$. We heuristically validate the approximation error by evaluating the error for $90 \cdot 10^3$ equidistant states on the domain \mathcal{X} , yielding a maximum error of $2.46 \cdot 10^{-3}$, i.e., about 50% smaller than the guaranteed error bound ϵ .

Figure 6 depicts the sub-domain partitioning of ALKIA-X, the feasible domain $\mathcal{X}_{\text{feas}}^f$ of the MPC, and $\mathcal{X}_{\text{feas}}^h$, the feasible domain computed by ALKIA-X. Recall that ALKIA-X partitions sub-domains further if the maximum number of samples

⁷Practical asymptotic stability implies convergence to a neighborhood of the steady-state x_s . In this case, the size of the neighborhood depends on the magnitude of the approximation error $\max_{x \in \mathcal{X}_{\text{feas}}^f} \|f(x) - h(x)\|_\infty \leq \epsilon$.

⁸Before executing ALKIA-X, we shift and scale the domain \mathcal{X} to yield the unit cube $[0, 1]^2$.

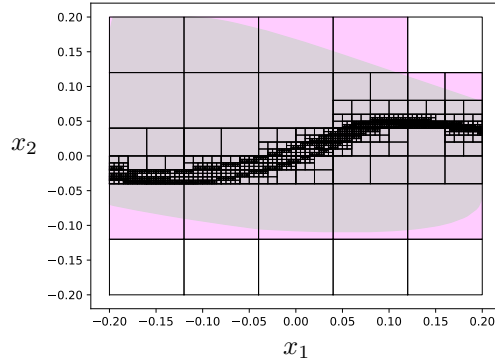


Fig. 6. Sub-domain partitioning using ALKIA-X and feasible domains. The light gray shaded area corresponds to the feasible domain $\mathcal{X}_{\text{feas}}^f$ of the ground truth MPC, whereas the area enclosed by the magenta shading corresponds to the feasible domain $\mathcal{X}_{\text{feas}}^h$ of the obtained approximate MPC via ALKIA-X. The resulting partitioning is reminiscent of classical linear explicit MPC approaches [26], [27]. In total, we have 1996 sub-domains.

cannot ensure the desired approximation error ϵ . This behavior can be observed in Figure 6, where larger sub-domains correspond to regions where the ground truth resembles a constant function (see Figure 5), and hence fewer samples are required. Furthermore, the derived sample complexities in Theorem 2 and Corollary 1 also support this statement.⁹ Overall, ALKIA-X successfully approximates the ground truth MPC f , yielding an approximate MPC h with closed-loop guarantees on stability and constraint satisfaction.

Discussion: In the following, we compare the MPC approximation obtained using ALKIA-X with the approach presented in [8]. Both works approximate the same ground truth MPC (see (48), Figure 5) with the identical error bound ϵ . ALKIA-X is a kernel-based algorithm that inherently guarantees the satisfaction of any desired error bound $\epsilon > 0$ (see Theorem 2, (P2), (P3)). In contrast, the approach in [8] uses NNs for the approximation and an additional statistical validation step to guarantee the desired approximation accuracy. Notably, the approach in [8] may lead to an *iterative* offline design between NN training and validation, e.g., requiring additional sampling or changes to the NN architecture whenever the statistical validation step fails.

Table I compares the number of samples $\text{card}(X)$, the offline approximation time t_{offline} , and the online evaluation time t_{online} of ALKIA-X and the NN approach proposed in [8].¹⁰ The online evaluation time of ALKIA-X is obtained over three runs of evaluating $90 \cdot 10^3$ equidistant states. Both ALKIA-X and the NN approach require roughly $\text{card}(X) \approx 10^6$ samples. However, the offline approximation time t_{offline} of [8] is significantly longer. The main reason for this discrepancy is that the NN approach requires further samples for the statistical validation step. Additionally, ALKIA-X yields an almost 100-

⁹The sample complexity on sub-domain \mathcal{X}_a increases with the RKHS norm $\|\tilde{f}_a\|_{\tilde{\kappa}_a}$ (see Theorem 2, Corollary 1). For constant functions, we have $\|\tilde{f}_a\|_{\tilde{\kappa}_a} = 0$.

¹⁰Table I directly contains the computation times reported in [8], which are not obtained with the same hardware as ALKIA-X.

	ALKIA-X	NN approach [8]
t_{online}	$44.02 \mu\text{s} \pm 0.14 \mu\text{s}$	$3000 \mu\text{s}$
t_{offline}	10.3 h	500 h
$\text{card}(X)$	$1.56 \cdot 10^6$	$1.6 \cdot 10^6$

TABLE I

COMPARISON BETWEEN ALKIA-X AND THE NN APPROXIMATION IN [8] WITH THE CONTINUOUS STIRRED TANK REACTOR.

times faster¹¹ online evaluation time t_{online} compared to the NN approach. The fast online evaluation of ALKIA-X (P1) is due to the *localized* kernel interpolation approach (T1), whereas standard kernel-based methods tend to suffer from scalability issues [34, Section 2.3].

In addition to the presented numerical differences, the closed-loop guarantees on the approximate MPC using ALKIA-X are *deterministic*. Furthermore, both the sample acquisition and the offline approximation of ALKIA-X are entirely parallelized, thus accelerating the offline approximation. Besides the favorable offline approximation time, the offline approximation with ALKIA-X is an *automatic* and *non-iterative* process (P4) in contrast to the iterative offline design present in [8].

B. Cold atmospheric plasma

We consider the MPC scheme to control a cold atmospheric plasma device from [46, Chapter 4.5]. The nonlinear systems dynamics $g: \mathbb{R}^3 \rightarrow \mathbb{R}^2$ are described by

$$g(x, u) = \begin{pmatrix} 0.427x_1 + 0.68x_2 + 1.58u_1 - 1.02u_2 \\ -0.06x_1 + 0.26x_2 + 0.73u_1 + 0.03u_2 \\ x_3 + \mathbb{K}^{(\mathbb{T}-x_1)}\delta \end{pmatrix}, \quad (49)$$

where x_1 is the surface temperature, x_2 is the gas temperature, and x_3 is the thermal dose delivered to the target surface. The inputs u_1 and u_2 correspond to the applied power to the plasma and the flow rate of Argon, respectively, while \mathbb{K} and \mathbb{T} are constants and $\delta = 0.5 \text{ s}$ is the sampling time. Note that states and inputs are appropriately shifted in (49), see [46, Chapter 4.5]. The state constraints⁸ are $x_1 \in [25^\circ\text{C}, 42.5^\circ\text{C}]$, $x_2 \in [20^\circ\text{C}, 80^\circ\text{C}]$, and $x_3 \in [0 \text{ min}, 11 \text{ min}]$, whereas the input constraints are $u_1 \in [1.5 \text{ W}, 8 \text{ W}]$ and $u_2 \in [1 \text{ slm}, 6 \text{ slm}]$. The control objective is to achieve a treatment time of the thermal dose of $\bar{x}_3 = 10 \text{ min}$ and satisfy the state and input constraints. The nonlinear MPC is formulated with a horizon of $N = 120$.

As mentioned in [46, Sections 1.2.2 and 6.2.2], approximate MPC schemes are desired for this application due the need for (i) sub-second sampling rates and (ii) implementability on portable embedded devices. To this end, we use ALKIA-X to determine an approximate MPC to control system (49). In this application example, we focus on obtaining an implementable controller for relatively cheap hardware with limited memory

¹¹More recently, [5] approximated the same ground truth MPC f with NNs, achieving an online evaluation time of $t_{\text{online}} = 500 \mu\text{s}$, which is still 10-times slower than the proposed solution. Furthermore, additional parallelization with 10^3 cores and the usage of GPUs reduced the offline sampling time to $t_{\text{offline}} = 0.5 \text{ h}$, resulting in $t_{\text{offline}} = 4.5 \text{ h}$ overall including the NN training. However, in contrast to the proposed approximation method, [5] does not guarantee error bound ϵ but utilizes a fallback policy to obtain closed-loop guarantees.

	Approximate MPC (ALKIA-X)	MPC (IPOPT)
t_{online}	$96 \mu\text{s} \pm 4 \mu\text{s}$	$507 \text{ ms} \pm 6 \text{ ms}$
Offline memory	33 MB	9 MB
t_{offline}	69 h	$[-]$
$\text{card}(X)$	$8.22 \cdot 10^5$	$[-]$

TABLE II

COMPARISON BETWEEN THE APPROXIMATE MPC COMPUTED BY ALKIA-X AND THE MPC WITH THE COLD ATMOSPHERIC PLASMA DEVICE.

capacities. Hence, instead of ensuring a desired error bound ϵ , we here focus on achieving the best approximation subject to a memory requirement on the samples of 75 MB, which we achieve by upper-bounding the maximum depth \bar{d} (see (47)) a priori. Specifically, for this application, we pre-partitioned the domain into 3^3 sub-domains and obtained $\bar{d} = 1$, i.e., each sub-domain can at most be partitioned into 2^3 further sub-domains. The hyperparameters for this experiment were $p = 2$ and $\bar{p} = 4$, yielding an upper bound on the condition number of $\bar{\kappa} = 3.32 \cdot 10^7$ (see (22), (31)).

Result: Table II compares the approximate MPC computed by ALKIA-X (Algorithm 4) and the MPC using online optimization (IPOPT) in terms of online evaluation time t_{online} , offline memory requirement, offline approximation time t_{offline} , and number of samples $\text{card}(X)$. The documented online evaluation times are obtained over three closed-loop runs of 30 time steps from the initial state $x = [35^\circ\text{C}, 58^\circ\text{C}, 0 \text{ min}]^\top$ and the NLP of the MPC is solved using a warm start. ALKIA-X requires a long time t_{offline} for the offline approximation¹², whereas the MPC only runs the just-in-time compilation prior to deployment. The offline memory requirements for the stored samples while executing ALKIA-X and for the compiled IPOPT code are comparable, both in the order of tens of megabytes. The benefit of the approximate MPC is the significant speedup of the online evaluation time t_{online} by a factor of over 10^3 .

Figure 7 illustrates the closed-loop trajectories of the MPC, where the NLP is solved using IPOPT, and of the approximate MPC computed by ALKIA-X. As in [46, Chapter 4.5], closed-loop simulations are terminated as soon as $x_3 \geq \bar{x}_3$. The trajectories are very similar, with x_3 showing no noticeable visual difference and all constraints are satisfied. Particularly, the approximation error between the approximate MPC and the MPC on the state trajectory of the approximate MPC is $\max_t \|f(x_t) - h(x_t)\|_\infty = 2.98 \cdot 10^{-3}$.

Overall, ALKIA-X (i) automatically computes an approximate MPC (P4) that closely resembles the MPC, (ii) reduces the online evaluation time by a factor of over 10^3 (P1), and (iii) only requires 33 MB of memory, thus being implementable on most microcontrollers.

VII. CONCLUSION

We addressed the problem of automatically approximating nonlinear MPC schemes while ensuring that the resulting approximate MPC inherits desirable closed-loop properties on stability and constraint satisfaction. By considering a robust

¹²Note that, due to parallelization, the offline approximation time can directly be reduced to $t_{\text{offline}} \approx 2.5 \text{ h}$ by increasing the number of cores from 8 to 216, provided sufficient RAM.

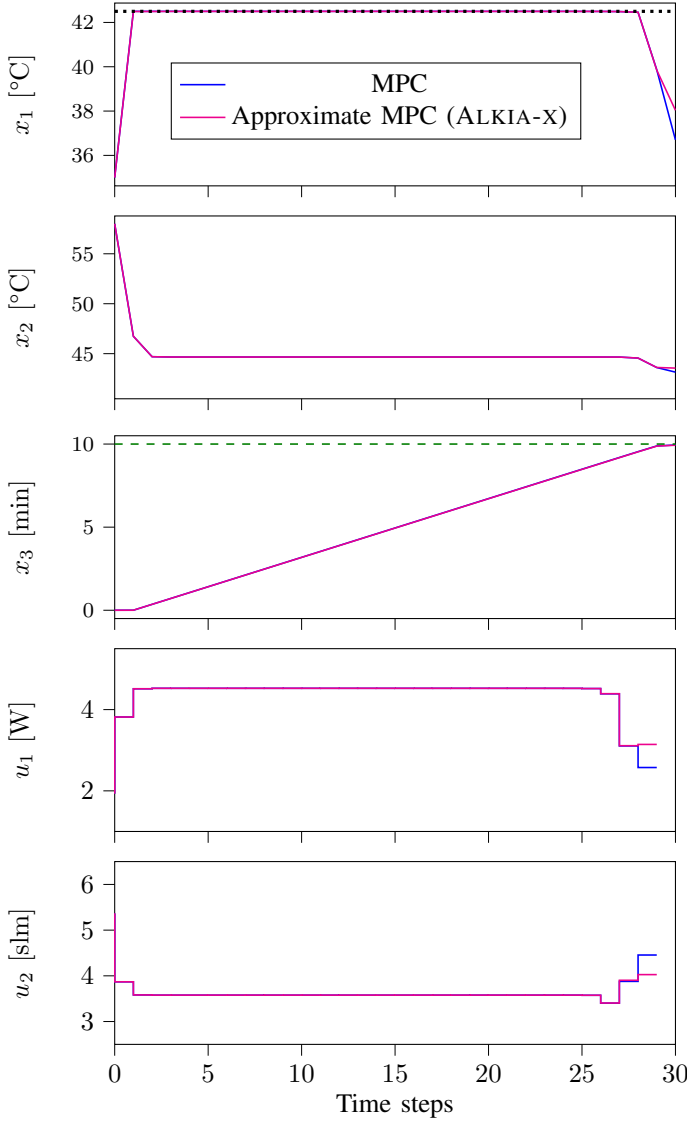


Fig. 7. Closed-loop state and input trajectories of the MPC (blue lines) and the approximate MPC (magenta lines) computed by ALKIA-X. The dotted black line shows the constraint on x_1 , whereas the dashed green line depicts the desired treatment time of $\bar{x}_3 = 10$ min.

MPC scheme, we reduced this problem to a function approximation problem, which we tackled by proposing ALKIA-X. ALKIA-X is an automatic and reliable algorithm that yields a computationally efficient approximate MPC with closed-loop guarantees. We successfully applied ALKIA-X to approximate two nonlinear MPC schemes, (i) demonstrating reduced offline computation and online evaluation time by over one order of magnitude and (ii) showcasing applicability to realistic problems with limited memory capacities.

Although we proposed ALKIA-X to approximate MPC schemes, the algorithm is equally capable of automatically approximating a wide range of black-box functions with guaranteed bounds on the approximation error.

ACKNOWLEDGEMENTS

The authors thank D. Baumann for helpful comments and J. Sieber for setting up the server.

APPENDIX A PROOF OF LEMMA 1

Analogous to [31, Proof of Lemma 4.23], for all $x, x' \in \mathcal{X}$, it holds that

$$\begin{aligned} |f(x) - f(x')| &= |\langle f, k(x, \cdot) - k(x', \cdot) \rangle_k| \\ &\leq \|f\|_k \sqrt{k(x, x) - k(x', x) - k(x, x') + k(x', x')} \\ &\stackrel{\text{Asm.1}}{=} \|f\|_k \sqrt{2 \left(1 - \tilde{k}(\|x - x'\|_2)\right)} \stackrel{(9)}{=} \|f\|_k \sqrt{2\mathfrak{K}(\|x - x'\|_2)}, \end{aligned}$$

where $\langle f, g \rangle_k$ denotes the inner product between two functions f, g in the RKHS of kernel k . The first equality follows from the reproducing property [31, Definition 4.18], while the first inequality follows from Cauchy-Schwarz. \square

APPENDIX B PROOF OF LEMMA 2

In Part I, we show that, for any $a \in \mathcal{A}$, (33) interpolates $\hat{\gamma}_{a,p}$ for $p \in \{\underline{p}, \underline{p} + 1\}$, i.e., (34) holds. In Part II, we prove that $\bar{\Gamma}_a \in (0, \infty)$ holds for any $a \in \mathcal{A}$.

Part I: Consider any $a \in \mathcal{A}$. First, we show $\gamma_a(\underline{p}) = \hat{\gamma}_{a,\underline{p}}$. It holds that

$$\begin{aligned} \gamma_a(\underline{p}) &\stackrel{(33)}{=} \bar{\Gamma}_a \exp\left(\frac{-\tau_a}{1 + 2^{\underline{p}}}\right) \\ &\stackrel{(35)}{=} \hat{\gamma}_{a,\underline{p}} \left(\frac{\hat{\gamma}_{a,\underline{p}+1}}{\hat{\gamma}_{a,\underline{p}}}\right)^\lambda \exp\left(\frac{-\ln\left(\frac{\hat{\gamma}_{a,\underline{p}+1}}{\hat{\gamma}_{a,\underline{p}}}\right) \lambda (1 + 2^{\underline{p}})}{1 + 2^{\underline{p}}}\right) \\ &= \hat{\gamma}_{a,\underline{p}} \left(\frac{\hat{\gamma}_{a,\underline{p}+1}}{\hat{\gamma}_{a,\underline{p}}}\right)^\lambda \exp\left(-\ln\left(\frac{\hat{\gamma}_{a,\underline{p}+1}}{\hat{\gamma}_{a,\underline{p}}}\right) \lambda\right) \\ &= \hat{\gamma}_{a,\underline{p}} \left(\frac{\hat{\gamma}_{a,\underline{p}+1}}{\hat{\gamma}_{a,\underline{p}}}\right)^\lambda \left(\frac{\hat{\gamma}_{a,\underline{p}}}{\hat{\gamma}_{a,\underline{p}+1}}\right)^\lambda = \hat{\gamma}_{a,\underline{p}}. \end{aligned}$$

Second, we show $\gamma_a(\underline{p} + 1) = \hat{\gamma}_{a,\underline{p}+1}$. It holds that

$$\begin{aligned} \gamma_a(\underline{p} + 1) &\stackrel{(33)}{=} \bar{\Gamma}_a \exp\left(\frac{-\tau_a}{1 + 2^{\underline{p}+1}}\right) \\ &\stackrel{(35)}{=} \hat{\gamma}_{a,\underline{p}} \left(\frac{\hat{\gamma}_{a,\underline{p}+1}}{\hat{\gamma}_{a,\underline{p}}}\right)^\lambda \exp\left(\frac{-\ln\left(\frac{\hat{\gamma}_{a,\underline{p}+1}}{\hat{\gamma}_{a,\underline{p}}}\right) \lambda (1 + 2^{\underline{p}})}{1 + 2^{\underline{p}+1}}\right) \\ &\stackrel{(32)}{=} \hat{\gamma}_{a,\underline{p}} \left(\frac{\hat{\gamma}_{a,\underline{p}+1}}{\hat{\gamma}_{a,\underline{p}}}\right)^\lambda \exp\left(\frac{-\ln\left(\frac{\hat{\gamma}_{a,\underline{p}+1}}{\hat{\gamma}_{a,\underline{p}}}\right) \lambda (1 + 2^{\underline{p}})}{2^{\underline{p}} \lambda}\right) \\ &= \hat{\gamma}_{a,\underline{p}} \left(\frac{\hat{\gamma}_{a,\underline{p}+1}}{\hat{\gamma}_{a,\underline{p}}}\right)^\lambda \exp\left(-\ln\left(\frac{\hat{\gamma}_{a,\underline{p}+1}}{\hat{\gamma}_{a,\underline{p}}}\right) (1 + 2^{-\underline{p}})\right) \\ &\stackrel{(32)}{=} \hat{\gamma}_{a,\underline{p}} \left(\frac{\hat{\gamma}_{a,\underline{p}+1}}{\hat{\gamma}_{a,\underline{p}}}\right)^\lambda \exp\left(-\ln\left(\frac{\hat{\gamma}_{a,\underline{p}+1}}{\hat{\gamma}_{a,\underline{p}}}\right) (\lambda - 1)\right) \\ &= \hat{\gamma}_{a,\underline{p}} \left(\frac{\hat{\gamma}_{a,\underline{p}+1}}{\hat{\gamma}_{a,\underline{p}}}\right)^\lambda \left(\frac{\hat{\gamma}_{a,\underline{p}}}{\hat{\gamma}_{a,\underline{p}+1}}\right)^{\lambda-1} \end{aligned}$$

$$= \hat{\gamma}_{a,\underline{p}} \left(\frac{\hat{\gamma}_{a,\underline{p}+1}}{\hat{\gamma}_{a,\underline{p}}} \right) = \hat{\gamma}_{a,\underline{p}+1},$$

i.e., (34) holds.

Part II: From (33), we have that $\bar{\Gamma}_a \in (0, \infty)$ if $\hat{\gamma}_{a,p} > 0$, $p \in \{\underline{p}, \underline{p}+1\}$ and $\hat{\gamma}_{a,\underline{p}+1} < \infty$. The fact that $\hat{\gamma}_{a,p} > 0$, $p \in \{\underline{p}, \underline{p}+1\}$ directly follows from (32) with $\epsilon > 0$. Moreover, from (33), it follows that $\hat{\gamma}_{a,\underline{p}+1} < \infty$ holds if $\|\tilde{h}_{X_{a,\underline{p}+1}}\|_{\tilde{k}_a} < \infty$ with $\epsilon < \infty$. Since the covariance matrix is always strictly positive definite (see Section II-B) and we have a continuous ground truth f on a bounded set \mathcal{X} (see Lemma 1), $\|\tilde{h}_{X_{a,\underline{p}+1}}\|_{\tilde{k}_a} < \infty$ follows from (30). \square

APPENDIX C PROOF OF LEMMA 3

For the SE-kernel $\tilde{k}_{\text{SE}}: \mathbb{R}_{\geq 0} \rightarrow [0, 1]$ with $\tilde{k}_{\text{SE}}(x) = \exp(-x^2)$ [34], we have $\mathfrak{R}_{\text{SE}}(x) = 1 - \exp(-x^2)$ (see (9)) and $\mathfrak{R}_{\text{SE}}^{-1}: [0, 1] \rightarrow \mathbb{R}_{\geq 0}$ with

$$\mathfrak{R}_{\text{SE}}^{-1}(x) = \sqrt{\ln\left(\frac{1}{1-x}\right)}. \quad (50)$$

With L'Hôpital's rule, it follows that

$$\frac{\ln\left(\frac{1}{1-x}\right)}{x} = \frac{1}{1-x} = 1, \quad \text{as } x \rightarrow 1. \quad (51)$$

Hence, (50) and (51) yield

$$\mathfrak{R}_{\text{SE}}^{-1}(x) = \sqrt{x}, \quad \text{as } x \rightarrow 1. \quad (52)$$

Thus, with (43), it holds for any $a \in \mathcal{X}_a$ that

$$\ell_a \leq \mathcal{O}\left(\frac{\sqrt{C}\epsilon}{\sqrt{n}\|f\|_k}\right) \quad \text{as } \frac{\epsilon}{\|f\|_k} \rightarrow 0,$$

which yields (45). \square

REFERENCES

- [1] J. B. Rawlings, D. Q. Mayne, and M. Diehl, *Model Predictive Control: Theory, Computation, and Design*. Nob Hill Publishing, 2017.
- [2] S. Chen, K. Saulnier, N. Atanasov, D. D. Lee, V. Kumar, G. J. Pappas, and M. Morari, "Approximating explicit model predictive control using constrained neural networks," in *Proc. Annual American Control Conference (ACC)*, 2018, pp. 1520–1527.
- [3] B. Karg and S. Lucia, "Efficient representation and approximation of model predictive control laws via deep learning," *IEEE Transactions on Cybernetics*, vol. 50, no. 9, pp. 3866–3878, 2020.
- [4] S. W. Chen, T. Wang, N. Atanasov, V. Kumar, and M. Morari, "Large scale model predictive control with neural networks and primal active sets," *Automatica*, vol. 135, p. 109947, 2022.
- [5] H. Hose, J. Köhler, M. N. Zeilinger, and S. Trimpe, "Approximate nonlinear model predictive control with safety-augmented neural networks," *arXiv preprint arXiv:2304.09575*, 2023.
- [6] X. Zhang, M. Bujarbaruah, and F. Borrelli, "Near-optimal rapid MPC using neural networks: A primal-dual policy learning framework," *IEEE Transactions on Control Systems Technology*, no. 5, pp. 2102–2114, 2021.
- [7] B. Karg, T. Alamo, and S. Lucia, "Probabilistic performance validation of deep learning-based robust NMPC controllers," *International Journal of Robust and Nonlinear Control*, vol. 31, no. 18, pp. 8855–8876, 2021.
- [8] M. Hertneck, J. Köhler, S. Trimpe, and F. Allgöwer, "Learning an approximate model predictive controller with guarantees," *IEEE Control Systems Letters*, vol. 2, no. 3, pp. 543–548, 2018.
- [9] J. Nubert, J. Köhler, V. Berenz, F. Allgöwer, and S. Trimpe, "Safe and fast tracking on a robot manipulator: Robust MPC and neural network control," *IEEE Robotics and Automation Letters*, vol. 5, no. 2, pp. 3050–3057, 2020.
- [10] G. Pin, M. Filippo, F. Pellegrino, G. Fenu, and T. Parisini, "Approximate model predictive control laws for constrained nonlinear discrete-time systems: analysis and offline design," *International Journal of Control*, vol. 86, no. 5, pp. 804–820, 2013.
- [11] T. Parisini, M. Sanguineti, and R. Zoppoli, "Nonlinear stabilization by receding-horizon neural regulators," *International Journal of Control*, vol. 70, no. 3, pp. 341–362, 1998.
- [12] C. Gonzalez, H. Asadi, L. Kooijman, and C. P. Lim, "Neural networks for fast optimisation in model predictive control: A review," *arXiv preprint arXiv:2309.02668*, 2023.
- [13] M. Canale, L. Fagiano, and M. Milanese, *Fast nonlinear model predictive control via set membership approximation: an overview*. Springer Berlin Heidelberg, 2009, vol. 12, pp. 461–470.
- [14] —, "Efficient model predictive control for nonlinear systems via function approximation techniques," *IEEE Transactions on Automatic Control*, vol. 55, no. 8, pp. 1911–1916, 2010.
- [15] M. Canale, L. Fagiano, and M. Signorile, "Nonlinear model predictive control from data: a set membership approach," *International Journal of Robust and Nonlinear Control*, vol. 24, no. 1, pp. 123–139, 2014.
- [16] M. Boggio, C. Novara, and M. Taragna, "Set membership based nonlinear model predictive control," *arXiv preprint arXiv:2212.12414*, 2022.
- [17] S. Ganguly and D. Chatterjee, "Explicit feedback synthesis driven by quasi-interpolation for nonlinear robust model predictive control," *arXiv preprint arXiv:2306.03027v1*, 2023.
- [18] M. Binder, G. Darivianakis, A. Eichler, and J. Lygeros, "Approximate explicit model predictive controller using Gaussian processes," in *Proc. 58th Conference on Decision and Control (CDC)*. IEEE, 2019, pp. 841–846.
- [19] A. Rose, M. Pfeifferkorn, H. H. Nguyen, and R. Findeisen, "Learning a Gaussian process approximation of a model predictive controller with guarantees," in *Proc. 62nd Conference on Decision and Control (CDC)*. IEEE, 2023, pp. 4094–4099.
- [20] B. Houska and M. E. Villanueva, *Robust Optimization for MPC*. Birkhäuser, 2019, pp. 413–443.
- [21] J. Köhler, R. Soloperto, M. A. Müller, and F. Allgöwer, "A computationally efficient robust model predictive control framework for uncertain nonlinear systems," *IEEE Transactions on Automatic Control*, vol. 66, no. 2, pp. 794–801, 2021.
- [22] A. Safi, M. N. Zeilinger, and J. Köhler, "Robust adaptive MPC using contraction metrics," *Automatica*, vol. 155, p. 111169, 2023.
- [23] S. V. Raković, L. Dai, and Y. Xia, "Homothetic tube model predictive control for nonlinear systems," *IEEE Transactions on Automatic Control*, vol. 68, no. 8, pp. 4554–4569, 2023.
- [24] A. Bemporad, M. Morari, V. Dua, and E. N. Pistikopoulos, "The explicit linear quadratic regulator for constrained systems," *Automatica*, vol. 38, pp. 3–20, 2002.
- [25] A. Alessio and A. Bemporad, *A Survey on Explicit Model Predictive Control*. Springer Berlin Heidelberg, 2009, pp. 345–369.
- [26] T. Johansen and A. Grancharova, "Approximate explicit constrained linear model predictive control via orthogonal search tree," *IEEE Transactions on Automatic Control*, vol. 48, no. 5, pp. 810–815, 2003.
- [27] S. Summers, C. N. Jones, J. Lygeros, and M. Morari, "A multiresolution approximation method for fast explicit model predictive control," *IEEE Transactions on Automatic Control*, vol. 56, no. 11, pp. 2530–2541, 2011.
- [28] A. Grancharova and T. A. Johansen, *Explicit Nonlinear Model Predictive Control: Theory and Applications*. Springer, 2012.
- [29] P. Scharnhorst, E. T. Maddalena, Y. Jiang, and C. N. Jones, "Robust uncertainty bounds in reproducing kernel Hilbert spaces: A convex optimization approach," *IEEE Transactions on Automatic Control*, vol. 68, no. 5, pp. 2848–2861, 2023.
- [30] E. T. Maddalena, P. Scharnhorst, and C. N. Jones, "Deterministic error bounds for kernel-based learning techniques under bounded noise," *Automatica*, vol. 134, p. 109896, 2021.
- [31] I. Steinwart and A. Christmann, *Support Vector Machines*. Springer, 2008.
- [32] G. M. Fasshauer and M. J. McCourt, *Kernel-based Approximation Methods using MATLAB*. World Scientific, 2015, vol. 19.
- [33] M. Kanagawa, P. Hennig, D. Sejdinovic, and B. K. Sriperumbudur, "Gaussian processes and kernel methods: A review on connections and equivalences," *arXiv preprint arXiv:1807.02582*, 2018.
- [34] C. E. Rasmussen and C. K. Williams, *Gaussian Processes for Machine Learning*. MIT Press, 2006.
- [35] H. Liu, Y.-S. Ong, X. Shen, and J. Cai, "When Gaussian process meets big data: A review of scalable GPs," *IEEE Transactions on Neural Networks and Learning Systems*, vol. 31, no. 11, pp. 4405–4423, 2020.

- [36] A. Lederer, A. J. O. Conejo, K. Maier, W. Xiao, J. Umlauf, and S. Hirche, "Real-time regression with dividing local Gaussian processes," *arXiv preprint arXiv:2006.09446*, 2020.
- [37] D. Nguyen-Tuong, J. Peters, and M. Seeger, "Local Gaussian process regression for real time online model learning and control," in *Proc. 21st Advances in Neural Information Processing Systems (NeurIPS)*, vol. 21, 2008.
- [38] F. Berkenkamp, A. Krause, and A. P. Schoellig, "Bayesian optimization with safety constraints: safe and automatic parameter tuning in robotics," *Machine Learning*, vol. 112, no. 10, pp. 3713–3747, 2023.
- [39] N. Srinivas, A. Krause, S. M. Kakade, and M. Seeger, "Information-theoretic regret bounds for Gaussian process optimization in the bandit setting," *IEEE Transactions on Information Theory*, vol. 58, no. 5, pp. 3250–3265, 2012.
- [40] S. R. Chowdhury and A. Gopalan, "On kernelized multi-armed bandits," in *Proc. 34th International Conference on Machine Learning (ICML)*. PMLR, 2017, pp. 844–853.
- [41] C. Fiedler, C. W. Scherer, and S. Trimpe, "Practical and rigorous uncertainty bounds for Gaussian process regression," in *Proc. 35th AAAI Conference on Artificial Intelligence*, no. 8, 2021, pp. 7439–7447.
- [42] Y. Sui, A. Gotovos, J. Burdick, and A. Krause, "Safe exploration for optimization with Gaussian processes," in *Proc. 32nd International Conference on Machine Learning*, vol. 37. JMLR, 2015, pp. 997–1005.
- [43] K. Hashimoto, A. Saoud, M. Kishida, T. Ushio, and D. V. Dimarogonas, "Learning-based symbolic abstractions for nonlinear control systems," *Automatica*, vol. 146, p. 110646, 2022, extended version on arXiv:1612.05327v3.
- [44] J.-P. Calliess, "Conservative decision-making and inference in uncertain dynamical systems," Ph.D. dissertation, University of Oxford, 2014.
- [45] M. Milanese and C. Novara, "Set membership identification of nonlinear systems," *Automatica*, vol. 40, no. 6, pp. 957–975, 2004.
- [46] A. D. Bonzanini, "Safe and fast learning-based model predictive control of nonlinear systems with applications to cold atmospheric plasma," Ph.D. dissertation, University of California, Berkeley, 2022.
- [47] H. K. Khalil, *Nonlinear Systems*. Patience Hall, 2002, vol. 115.
- [48] T. Kailath, "RKHS approach to detection and estimation problems—Part I: Deterministic signals in Gaussian noise," *IEEE Transactions on Information Theory*, vol. 17, no. 5, pp. 530–549, 1971.
- [49] T. Kailath, R. Geesey, and H. Weinert, "Some relations among RKHS norms, Fredholm equations, and innovations representations," *IEEE Transactions on Information Theory*, vol. 18, no. 3, pp. 341–348, 1972.
- [50] H. Pradhan, A. Koppel, and K. Rajawat, "On submodular set cover problems for near-optimal online kernel basis selection," in *International Conference on Acoustics, Speech and Signal Processing (ICASSP)*. IEEE, 2022, pp. 4168–4172.
- [51] E. C. Kerrigan and J. M. Maciejowski, "Soft constraints and exact penalty functions in model predictive control," in *UKACC International Conference (Control 2000)*, 2000.
- [52] E. Rosenberg, "Exact penalty functions and stability in locally Lipschitz programming," *Journal of Optimization Theory and Applications*, vol. 30, pp. 340–356, 1984.
- [53] J. A. E. Andersson, J. Gillis, G. Horn, J. B. Rawlings, and M. Diehl, "CasADi – A software framework for nonlinear optimization and optimal control," *Mathematical Programming Computation*, vol. 11, no. 1, pp. 1–36, 2019.
- [54] A. Wächter and L. T. Biegler, "On the implementation of an interior-point filter line-search algorithm for large-scale nonlinear programming," *Mathematical Programming*, vol. 106, pp. 25–57, 2006.



Abdullah Tokmak received his B.Sc. and M.Sc. degrees in mechanical engineering from RWTH Aachen University, Aachen, Germany, in 2020 and 2022, respectively. In 2022, he received the Springorium Commemorative Coin for his Master's degree and the Friedrich-Wilhelm Award for his Master's thesis, both from RWTH Aachen University. He is currently a doctoral researcher at the Cyber-physical Systems Group of Aalto University, Espoo, Finland. His research interests include machine learning and control.



Christian Fiedler Christian Fiedler received the B.Sc. degree in Mathematics from the University of Bayreuth in 2015, the M.Phil. degree in Computational Biology from the University of Cambridge in 2017, and the M.Sc. degree in Mathematics from the Technical University of Munich. During his studies, he was supported by the Max Weber program. In 2019, he joined the Max Planck Institute for Intelligent Systems and the University of Stuttgart as a PhD student, before transferring to RWTH Aachen University in 2021. He has broad research interests

at the intersection of control theory and machine learning, with a particular focus on kernel methods.



Melanie N. Zeilinger is an Associate Professor at ETH Zurich, Switzerland. She received the Diploma degree in engineering cybernetics from the University of Stuttgart, Germany, in 2006, and the Ph.D. degree with honors in electrical engineering from ETH Zurich, Switzerland, in 2011. From 2011 to 2012 she was a Postdoctoral Fellow with the Ecole Polytechnique Federale de Lausanne (EPFL), Switzerland. She was a Marie Curie Fellow and Postdoctoral Researcher with the Max Planck Institute for Intelligent Systems, Tübingen, Germany

until 2015 and with the Department of Electrical Engineering and Computer Sciences at the University of California at Berkeley, CA, USA, from 2012 to 2014. From 2018 to 2019 she was a professor at the University of Freiburg, Germany. She was awarded the ETH medal for her PhD thesis, an SNF Professorship, the ETH Golden Owl for exceptional teaching in 2022 and the European Control Award in 2023. Her research interests include learning-based control with applications to robotics and human-in-the-loop control.



Sebastian Trimpe Sebastian Trimpe received the B. Sc. degree in general engineering science and the M. Sc. degree (Dipl.-Ing.) in electrical engineering from Hamburg University of Technology, Hamburg, Germany, in 2005 and 2007, respectively, and the Ph. D. degree (Dr. sc.) in mechanical engineering from ETH Zurich, Zurich, Switzerland, in 2013. Since 2020, he is a full professor at RWTH Aachen University, Germany, where he heads the Institute for Data Science in Mechanical Engineering. Before, he was an independent Research Group Leader at

the Max Planck Institute for Intelligent Systems in Stuttgart and Tübingen, Germany. His main research interests are in systems and control theory, machine learning, networked systems and robotics. Dr. Trimpe has received several awards, including the triennial IFAC World Congress Interactive Paper Prize (2011), the Klaus Tschira Award for achievements in public understanding of science (2014), the Best Paper Award of the International Conference on Cyber-Physical Systems (2019), and the Future Prize by the Ewald Marquardt Stiftung for innovations in control engineering (2020).



Johannes Köhler received his Master degree in Engineering Cybernetics from the University of Stuttgart, Germany, in 2017. In 2021, he obtained a Ph.D. in mechanical engineering, also from the University of Stuttgart, Germany, for which he received the 2021 European Systems & Control PhD award. He is currently a postdoctoral researcher at ETH Zürich. His research interests are in the area of model predictive control and control and estimation for nonlinear uncertain systems.